Polywell Fusion
Electrostatic Fusion in a Magnetic Cusp

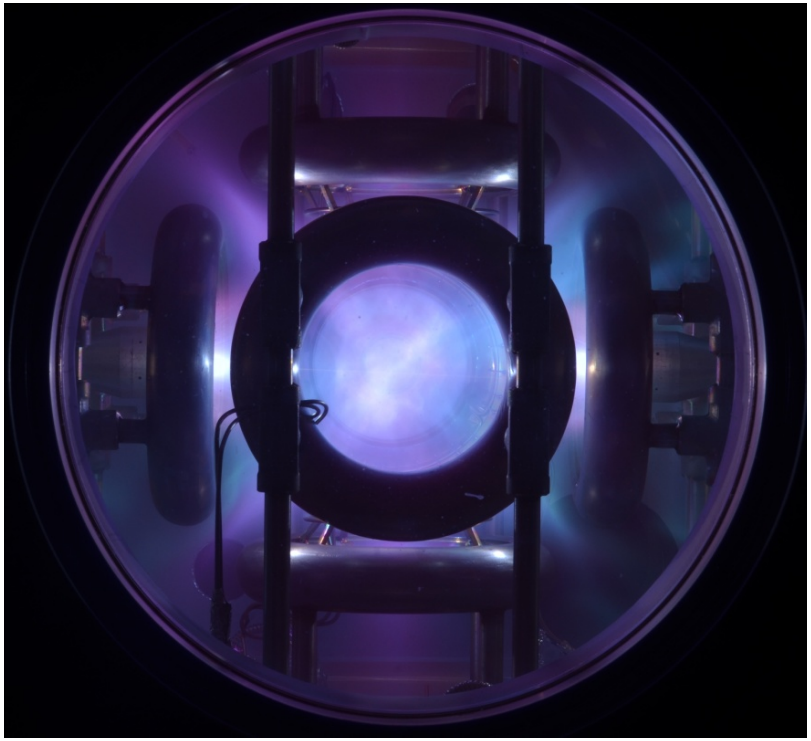

Jaeyoung Park
Energy Matter Conversion Corporation (EMC2)
Fusion Power Associates Meeting (December 17, 2014)
Support from US Navy Contract: N68936-09-C-0125

Contributions from EMC2 Personnel

4 Scientists, 5 Engineers/Technicians, 2 Support

Mike Skillicorn: Design, construction and maintenance of WB-8 device

Paul Sieck: WB-8 operation, control and safety system, and DAQ

Dustin Offermann: Plasma diagnostics – Spectroscopy, lasers and x-ray

Eric Alderson: Plasma diagnostics – Probes and particle diagnostics

Mike Wray: Vacuum and gas handling system and lab Management

Noli Casama: Electrical power system

Kevin Davis: Microwave system and HV pulse power operation

Andy Sanchez: Operation Support and Numerical Simulation

Grace Samodal: Business/Operations Management

Yoko Corniff: Accounting and HR

Jaeyoung Park: Lead the WB-8 project

EMC2 works closely with Dr. Nicholas A. Krall on Polywell theory

Contributors to the Polywell Fusion Concept

Philo Farnsworth
Electric fusion & inventor of television

Harold Grad
MHD theory and Cusp confinement

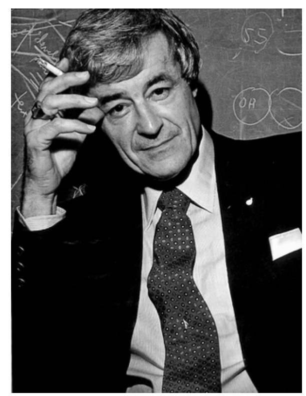

Robert Bussard
Polywell Fusion, Nuclear Rocket, Bussard Ramjet

James Tuck: Picket Fence, Elmore-Tuck-Watson virtual cathode, & Explosive focus for A-bomb

Polywell Fusion Principle

Combines two good ideas in fusion research: Bussard (1985)

a) **Electrostatic fusion:** High energy electron beams form a potential well, which accelerates and confines ions.

b) **High β magnetic cusp**: High energy electron confinement in high β cusp: Bussard termed this as "wiffle-ball" (WB).

Electrostatic fusion provides
- Ion heating
- Ion confinement

for high β cusp

High β cusp provides
- High energy electron confinement

for electrostatic fusion

Polywell Cusp Magnetic Fields

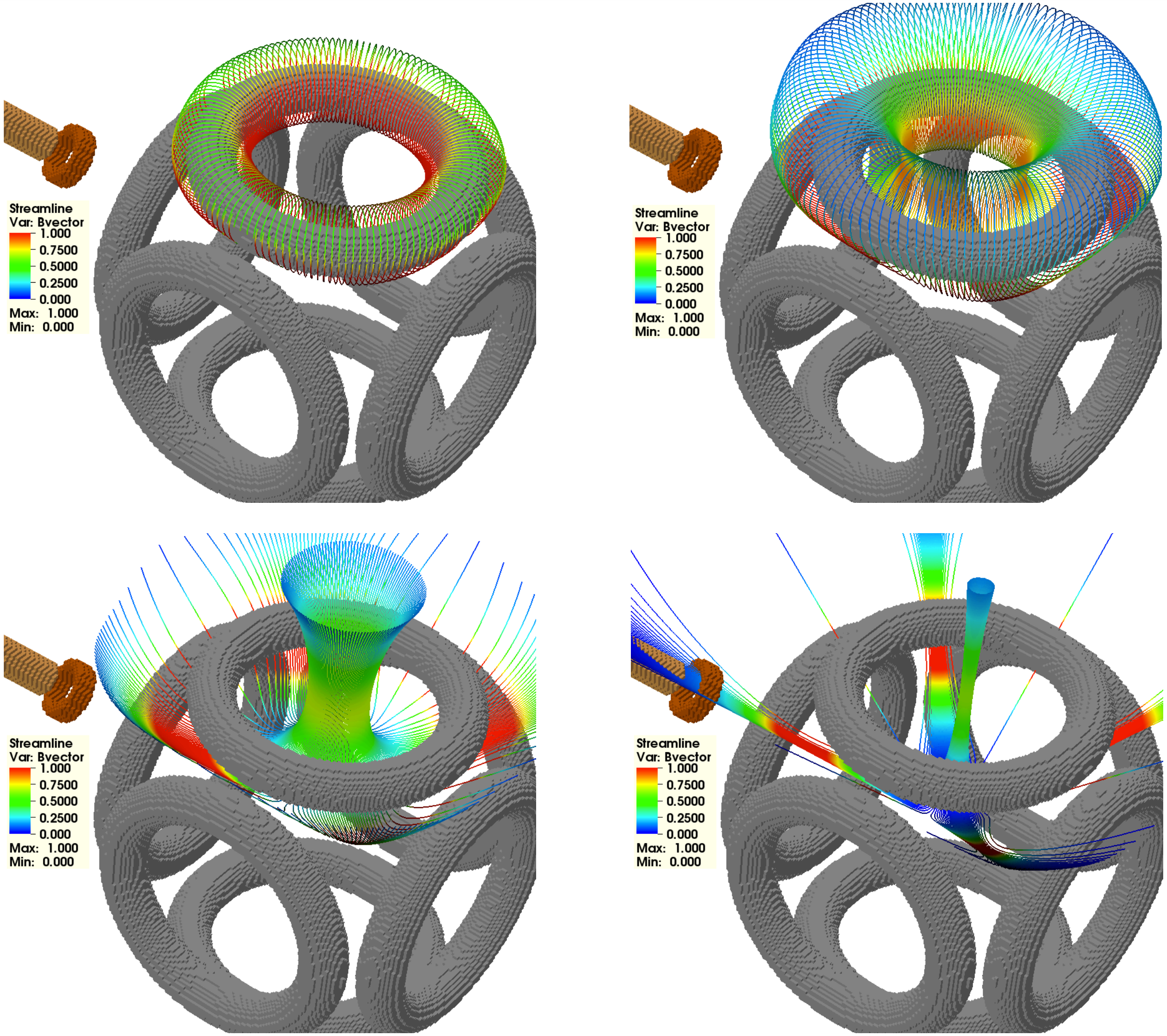

- ***6 coil Polywell cusp magnetic field lines***
- ***Electron beam injection along the cusp openings***

Potential Well by e-beam Injection (1995)

at low plasma density

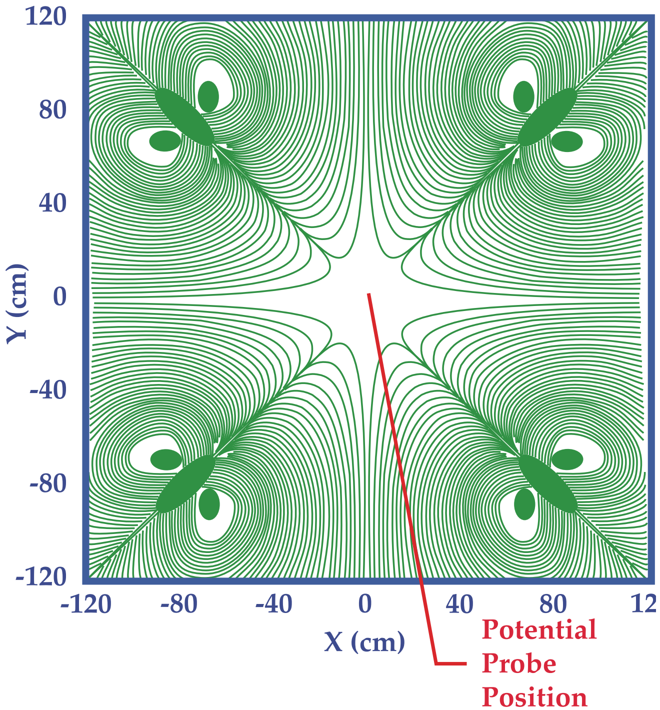

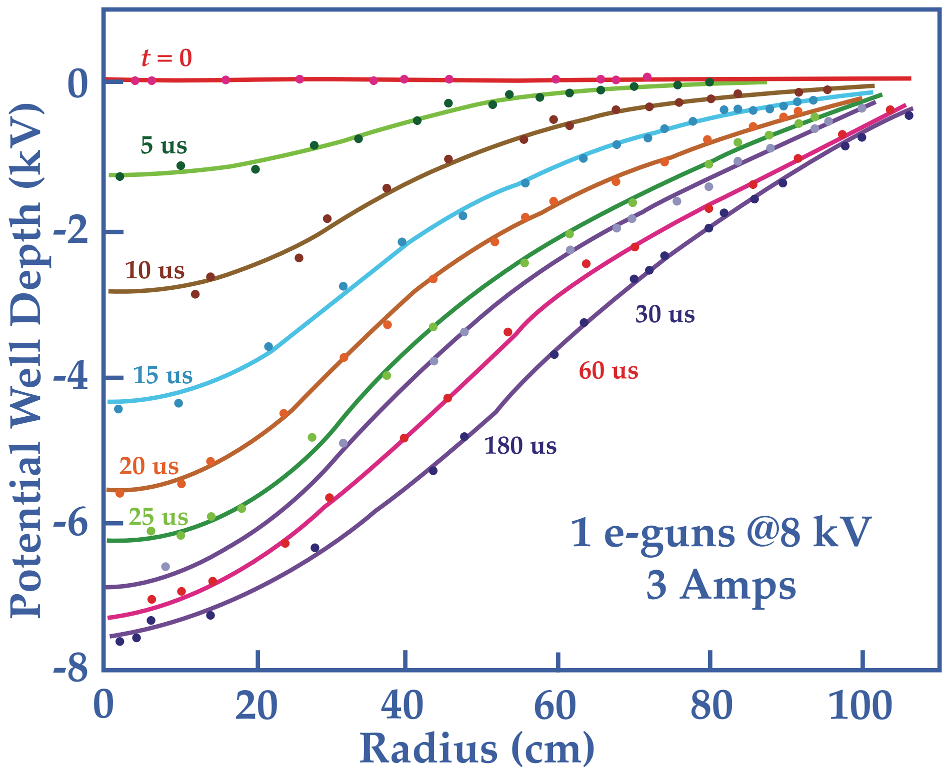

However, the potential well decayed away with increase in plasma density above $1x10^9$ cm^{-3}, which was contributed to the insufficient confinement of fast electrons inside the Polywell cusp field (*Krall et al, Physics of Plasmas, 1995)*

Progression of EMC2 Polywell Devices

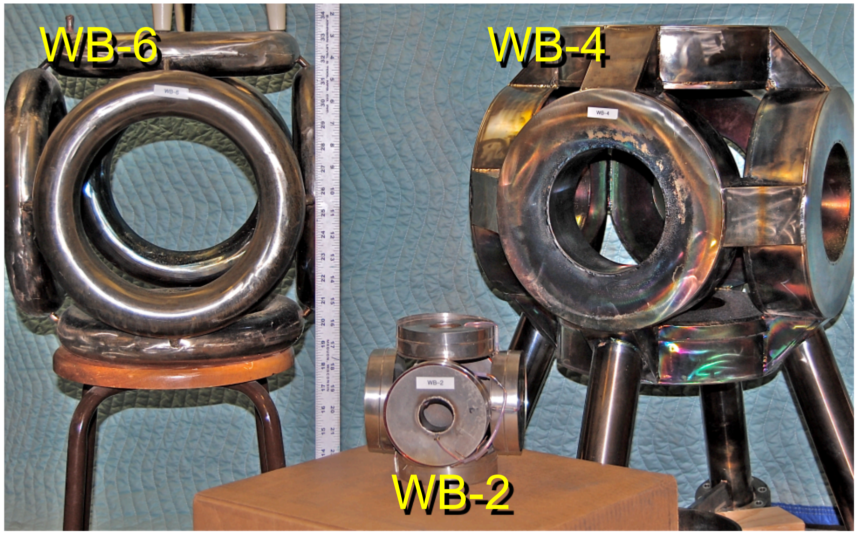

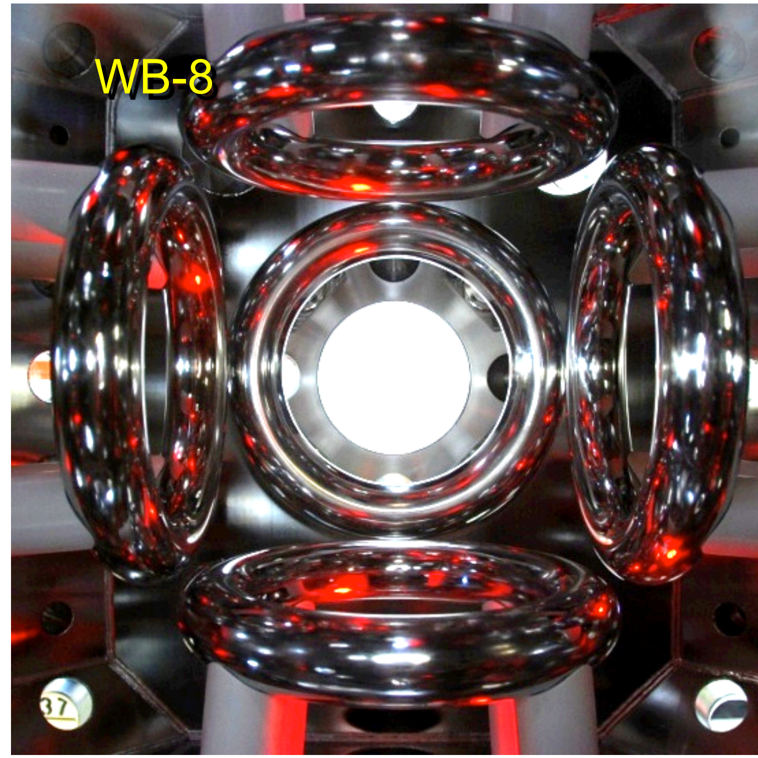

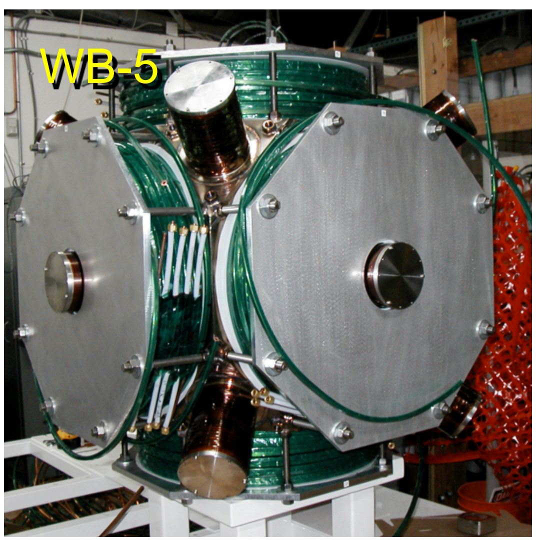

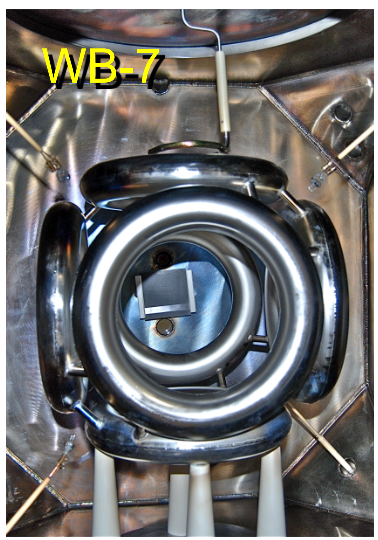

Since 1994, EMC2 had built and operated successive test devices from Wiffle-Ball-1 (WB-1) to WB-8 to demonstrate confinement of high energy electrons in a magnetic cusp.

Motivation of Magnetic Cusp

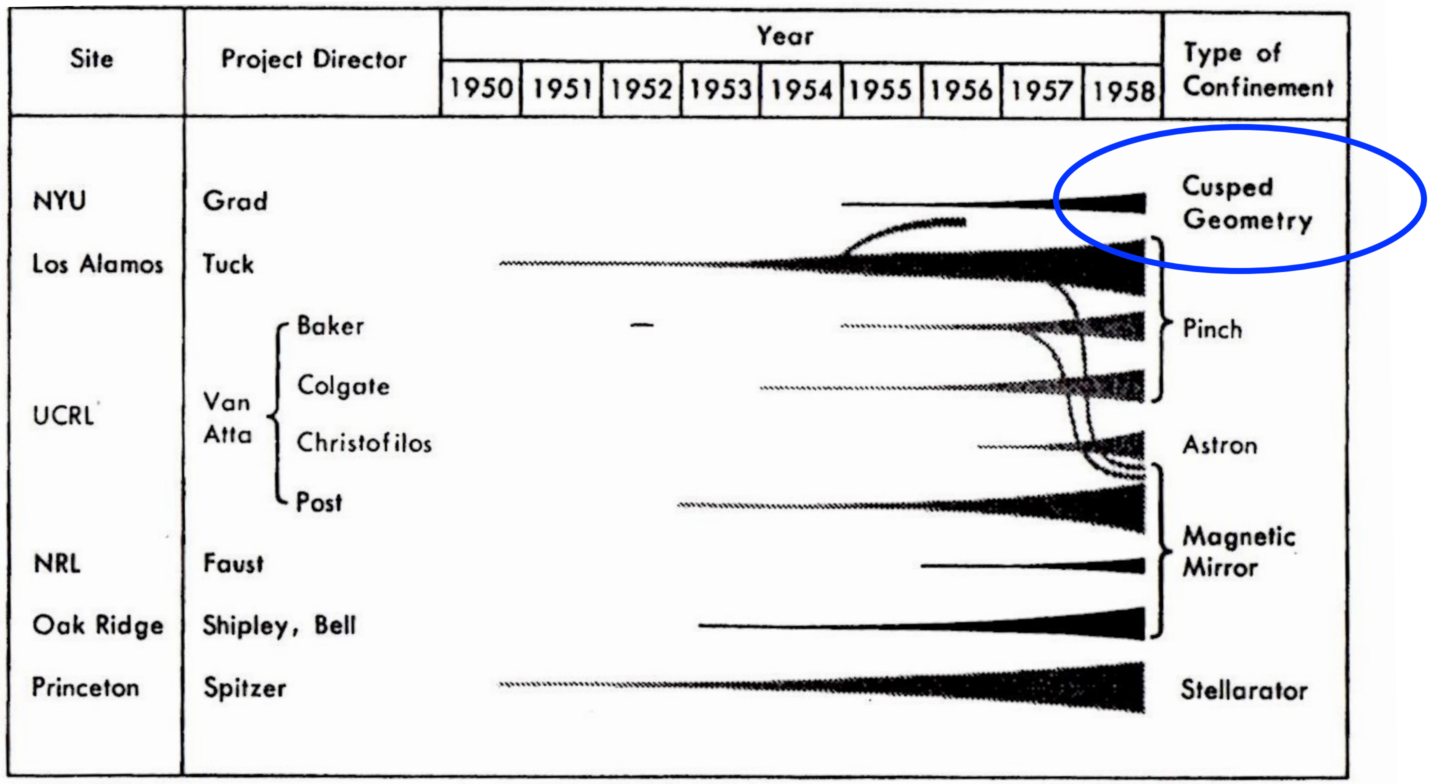

FIG. 19–2. CHRONOLOGY OF THE SHERWOOD PROGRAM, showing methods of plasma confinement in experiments to date.

Magnetic cusp was introduced to magnetic fusion program for plasma stability and high beta (β=1) operation

From "Project Sherwood: The U. S. Program in Controlled Fusion" by Amasa Bishop (1958).

Grad's High Beta Cusp Conjecture

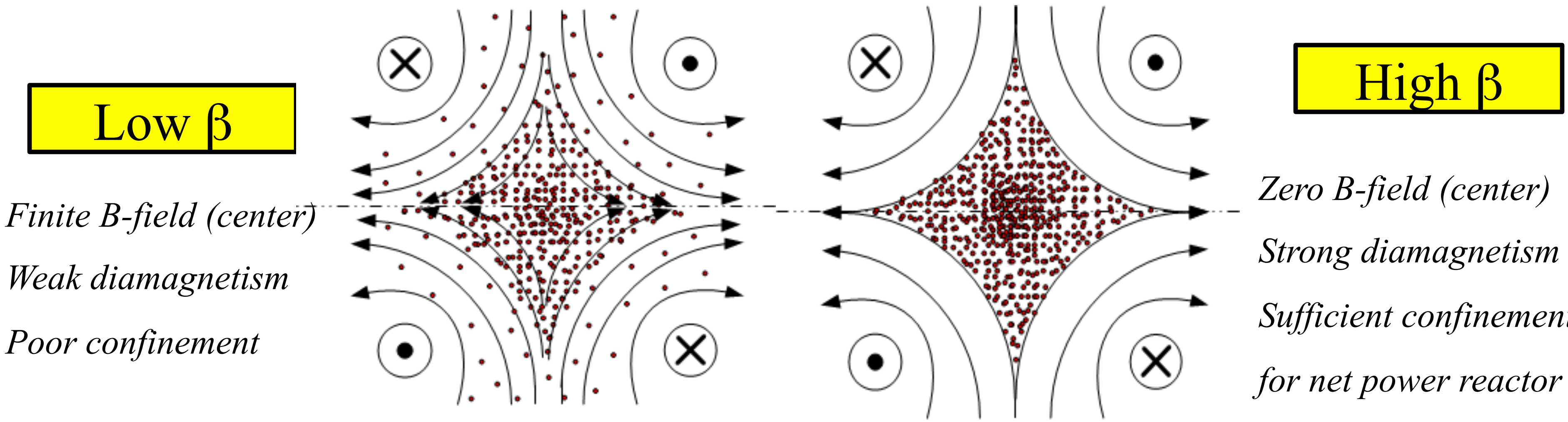

- Between 1955-1958, NYU group led by Grad investigated the case of plasma confinement in a high β magnetic cusp.
- In Grad's view, a boundary between plasma and magnetic fields are very different for low β and high β case.
- For high β cusp, he envisioned "**a sharp transition layer to exist between plasma and B-fields, while diamagnetic effect results in a field free central region**"
- Plasma particles will undergo specular reflection at the boundary except for the particle moving almost exactly in the direction of the cusp → **the plasma loss rate will be greatly reduced and have gyro-radius scaling.**

Plasma Confinement in Cusp at High β

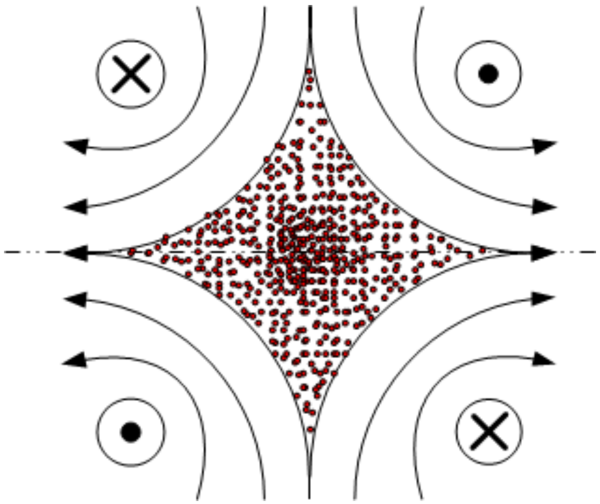

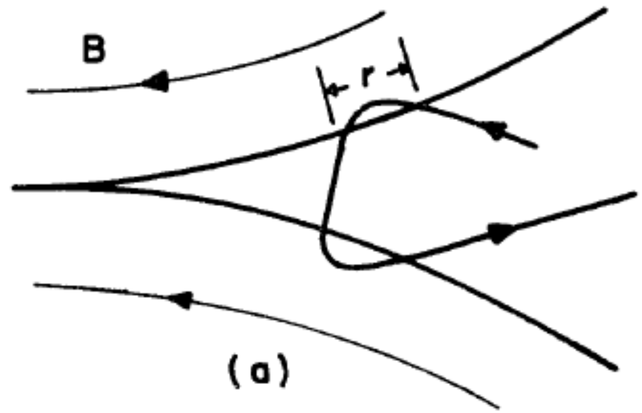

Berkowitz et al
1958 paper
"Cusped geometries"

In high β cusp, **a sharp transition layer exists between plasma and B-fields**. Plasma particles will undergo specular reflection at the boundary except for the particle moving almost exactly in the direction of the cusp. The loss rate will have gyro-radius scaling.

Theoretically conjectured

Loss current per cusp by Grad and NYU team

$$\frac{I_{e,i}}{e} = \frac{\pi}{9} n_{e,i} v_{e,i} \times \pi (r_{e,i}^{gyro})^2$$

0.5s confinement time
for 100 keV electron with 7 T, 1m radius, 6 coil cusp → favorable for a net power device.

History of Cusp Confinement Efforts

- Grad's confinement enhancement conjecture made the cusp approach to be promising for a net power fusion reactor.

- For the next 20 years, detailed experiments were conducted on ~20 different devices and ~200 papers were published related to the cusp confinement as a result. Two excellent review articles by Spalding (1971) and Haines (1977).

- However, most efforts on cusp confinement stopped by 1980 due to a lack of progress.

High Beta Cusp Experiments in 1960s

using plasma injection

TABLE I

Typical Injection—Cusp Experiments[a]

References	Plasma source; confinement geometry	Diameter D (cm)	Length L(cm)	B (max) (kG)	n_e cm^{-3}	W'' keV	T_e eV	Quoted β near axis
67	Single-pulse coaxial gun; axisymmetric quadrupole and octupole	90	120	4.5	10^{12}–10^{14}	5×10^{-2}	15	?
68	12 conical Z-pinch guns; axisymmetric triple cusp (radial injection)	20	45	1.9	7.5×10^{14}	$>5 \times 10^{-3}$	4.5	<1
69	Coaxial gun; spindle-cusp	53	53	12	$\sim 3 \times 10^{13}$	13	Nonthermal	<1/2
70, 71	2 θ-Pinch (single pulse) guns; spindle cusp	25	230	3.2	$\sim 10^{15}$	2.4×10^{-1}	20	$\gg 0.90$ in core
72	Conical Z-pinch; spindle cusp	40	40	4	$(3–10) \times 10^{15}$	~ 1	?	~ 1
73	Titanium guns; spindle cusp (radial injection)	12	12	3.9	$\sim 8 \times 10^{15}$	5×10^{-2}	>5	~ 1
74	2 multiple-pulse coaxial guns; spindle cusp	17	15	3.9	10^{13}	2×10^{-2}	6	~ 1

[a] Axial injection unless radial injection at ring cusps is specifically noted. W'' is the injected energy in keV.

102

Cont. High Beta Cusp Experiments in 1960s

using plasma compression

TABLE II
Recent Compression—Cusp Experiments

Refs.	Description	D (cm)	L (cm)	B kg	Rise time (μsec)	$\hat{n}$ (cm^{-3})	$\hat{Te}$ eV	β_A
75	Adiabatic spindle cusp	11	8	25	4.5	?	?	?
76–78	Ditto (shock preheat)	20	20	24	15	$2{\cdot}5 \times 10^{16}$	15	0.98
79	Ditto (gun preheat)	20	20	34	15	10^{16}	70	~1·0
80	Shock-heated spindle cusp	10·5	13	70	1·1	10^{17}	120	?
81	Linear θ-cusp-θ pinch	5	2·5	27	1	$\sim 3 \times 10^{16}$	100–180	?
82–84	Shock-heated linear cusp-θ-cusp pinch	19	50	60	2·1	$1{\cdot}5 \times 10^{16}$	150	0.99 ± 0.01
85	Shock-heated toroidal hexapole	6	163	10	3·0	3×10^{16}	50	0·8
86	Shock-heated toroidal hexapole	6 6	163 163	21 10·5	3·0 3·0	$3{\cdot}5 \times 10^{16}$ $1{\cdot}4 \times 10^{16}$	93 62	0·4 1·0

From review article by I. Spalding, "Cusp Containment" In Advances in Plasma Physics.
(A. Simon, W. B. Thompson, Eds., Wiley, New York, 1971)

Recent Experiments at EMC2
(EMC2 San Diego Facility)

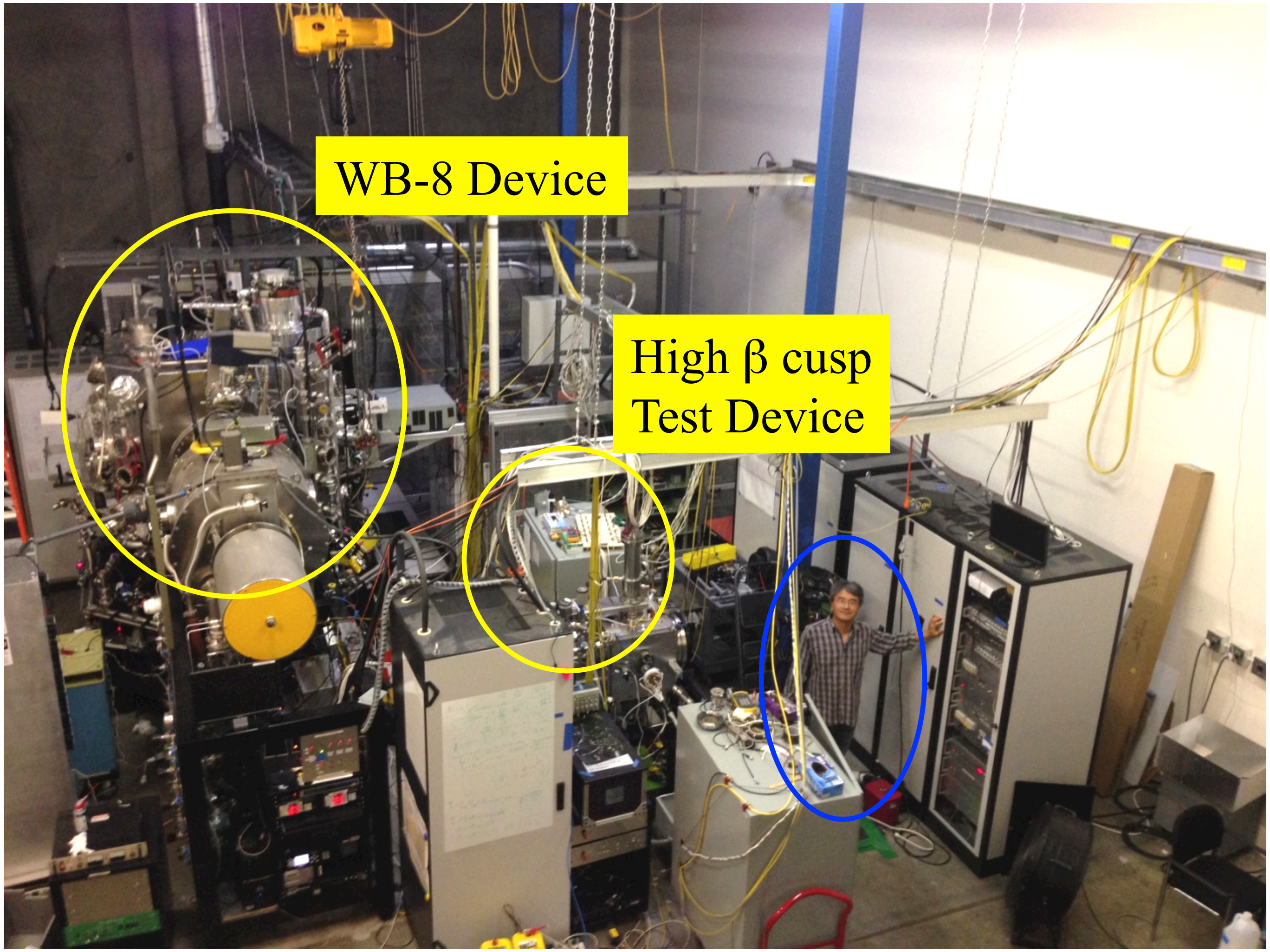

EMC2 Experimental Plan

1. Plasma injection to the cusp
   - Use high power arc (solid target) plasma injectors
2. Verify high β plasma formation in the cusp
   - Measurements on plasma density, magnetic flux and electron temperature
3. High energy electron injection to high β cusp
   - LaB_6 based electron beam injector, used as fast test particles.
4. Confinement measurement of high energy electrons in the cusp
   - Time resolved hard x-ray intensity from bremsstrahlung

Bulk (cold & dense) plasma from arc injectors provides plasma pressure (high β) to modify cusp B-fields, while the confinement property is measured for high energy electrons in the cusp.

First ever confirmation of high β cusp confinement enhancement (October 23, 2013)

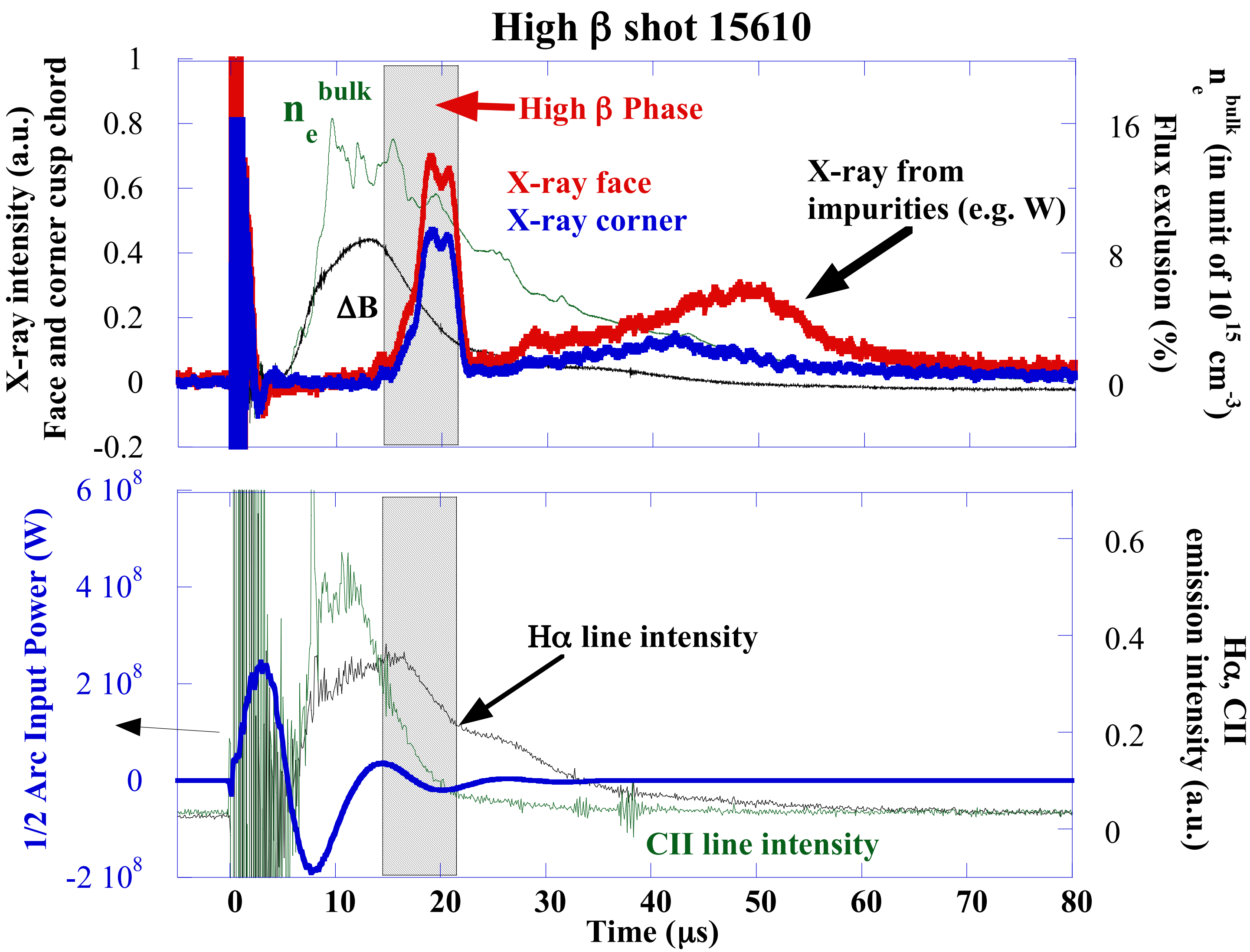

Cusp confinement vs. Injection input power

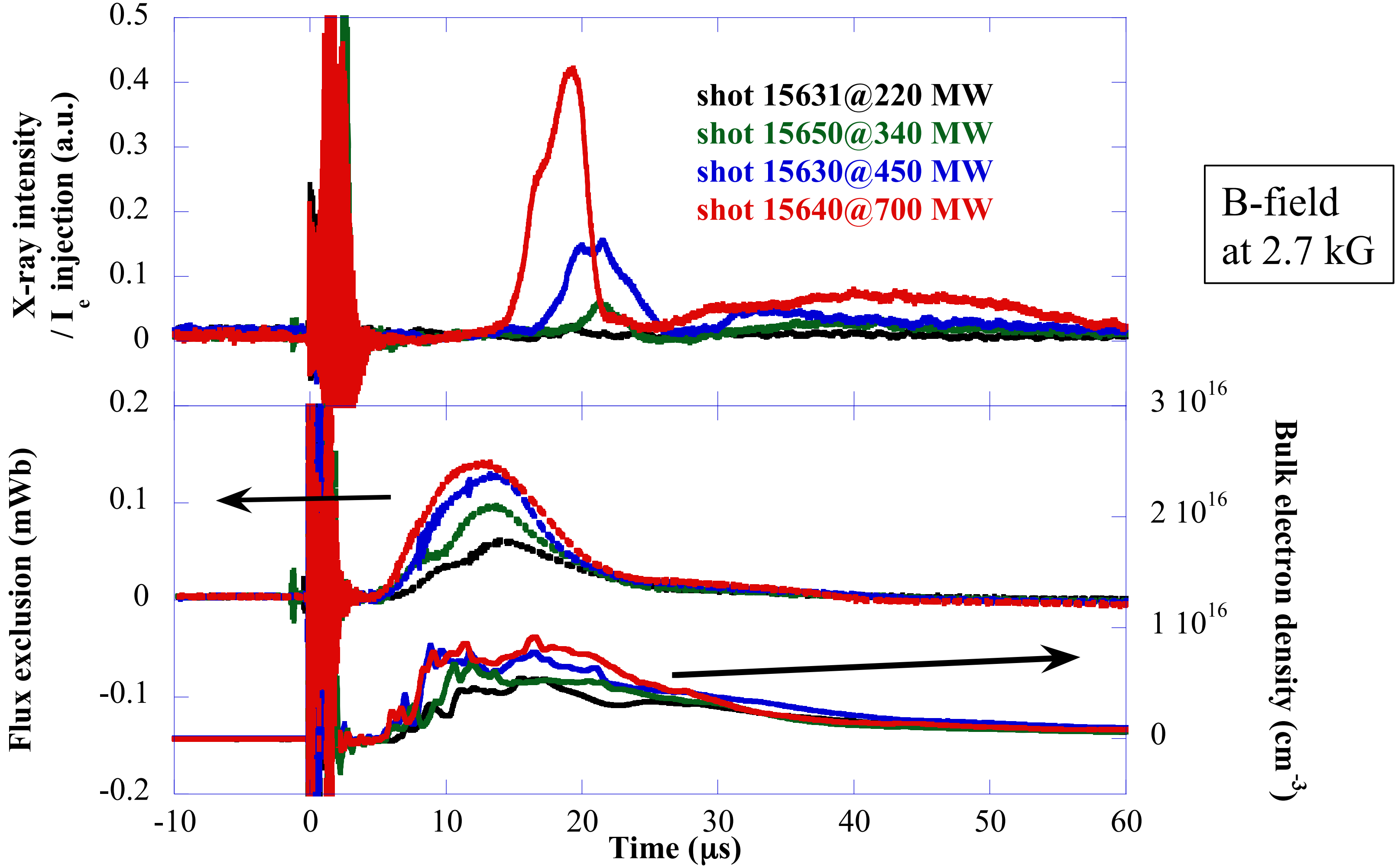

<u>Cusp confinement enhancement requires sufficiently high β plasma condition</u>

Cusp confinement vs. initial B-fields

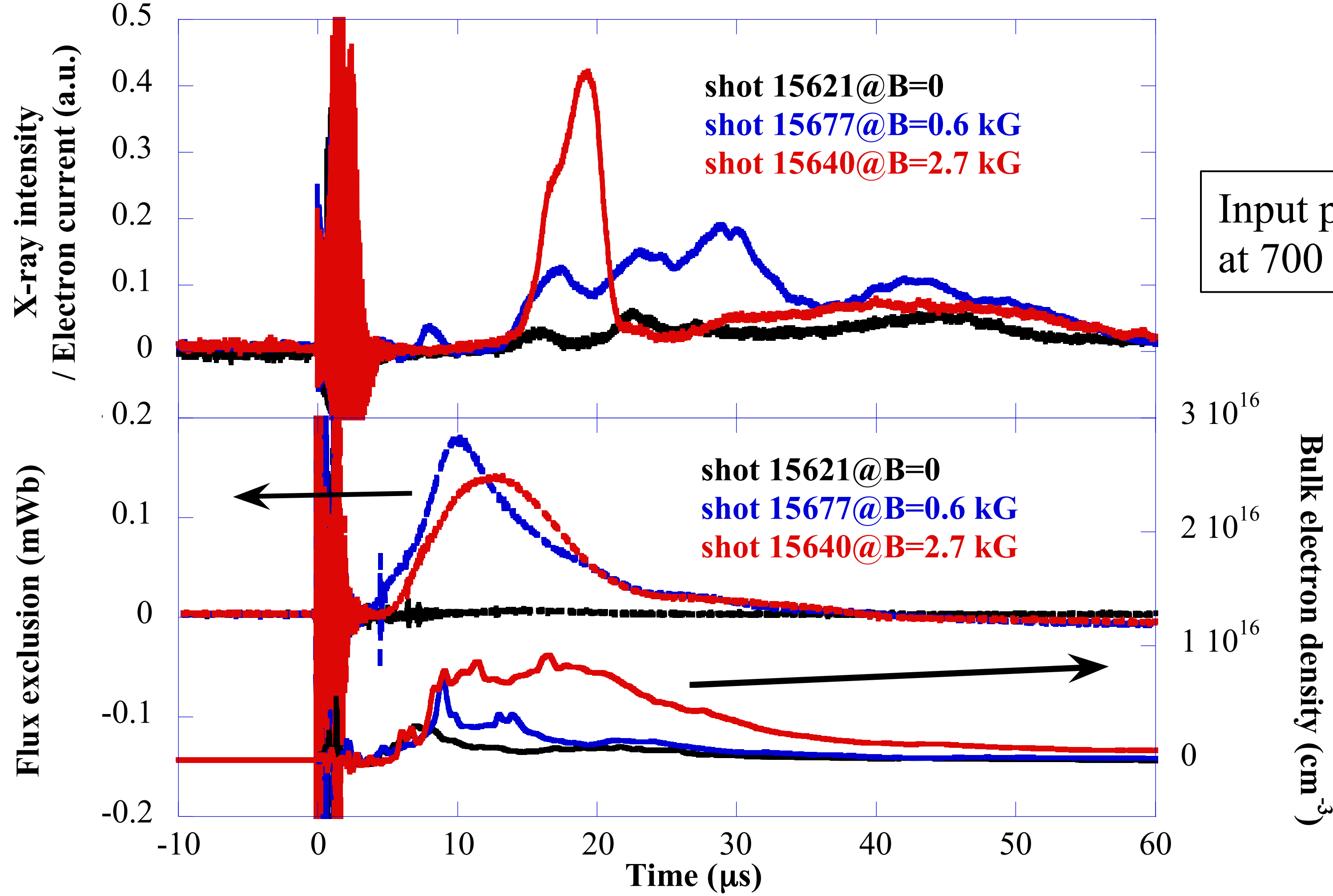

Input power at 700 MW

No confinement enhancement at B=0 but we need to do more to understand B-field effects

Our Findings on High β Cusp Confinement

Increase in X-ray signal

- Coincides with high β plasma state in the cusp
- Only observed when there is sufficient flux exclusion or plasma injection reaches a threshold
- Peak increase is 10-20x or more compared to low β state
- Exhibits asymmetrical time behavior: gradual increase followed by rapid decrease
- Clearly separated from W impurities injection in time domain

We believe our x-ray measurements unambiguously validate the enhanced electron confinement in a high β cusp compared to a low β cusp

Technical paper submitted to Physical Review X and preprint available on arXiv:1406.0133 (2014)

A Path to Polywell Fusion

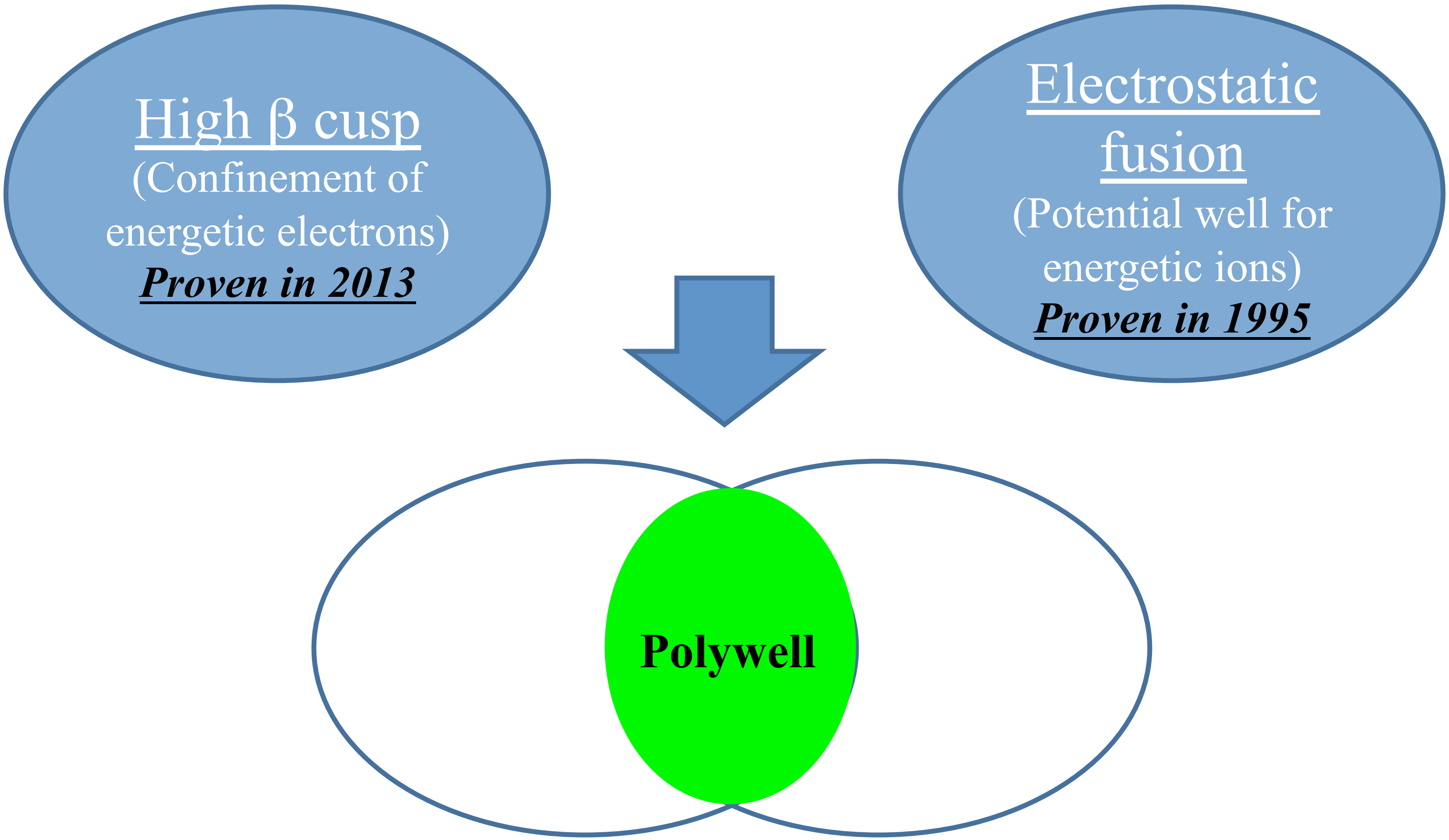

High β cusp + Electrostatic fusion at the same time

Merits of Polywell Fusion Reactor

Scientific merits

- MHD stability
- High β operation
- Electrostatic heating of ions
- No helium ash issue

Engineering merits

- Compact size
- Heating by electron beam injection
- Natural divertor
- Modular, non-interlocking coils
- Remote first wall

Polywell fusion may offer a low cost and rapid development path

Movie of Polywell Fusion Reactor Assembly

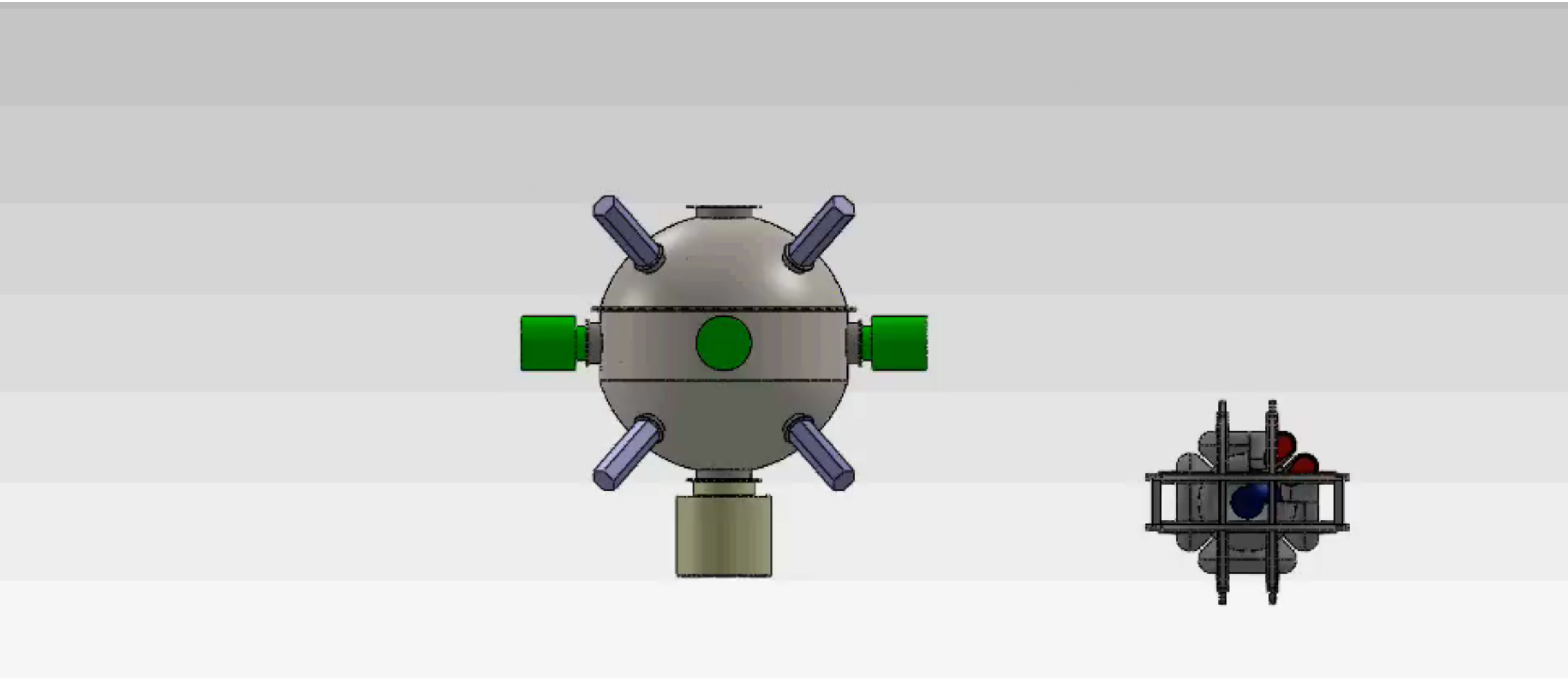

Next Phase: Last Part of Proof-of-Principle

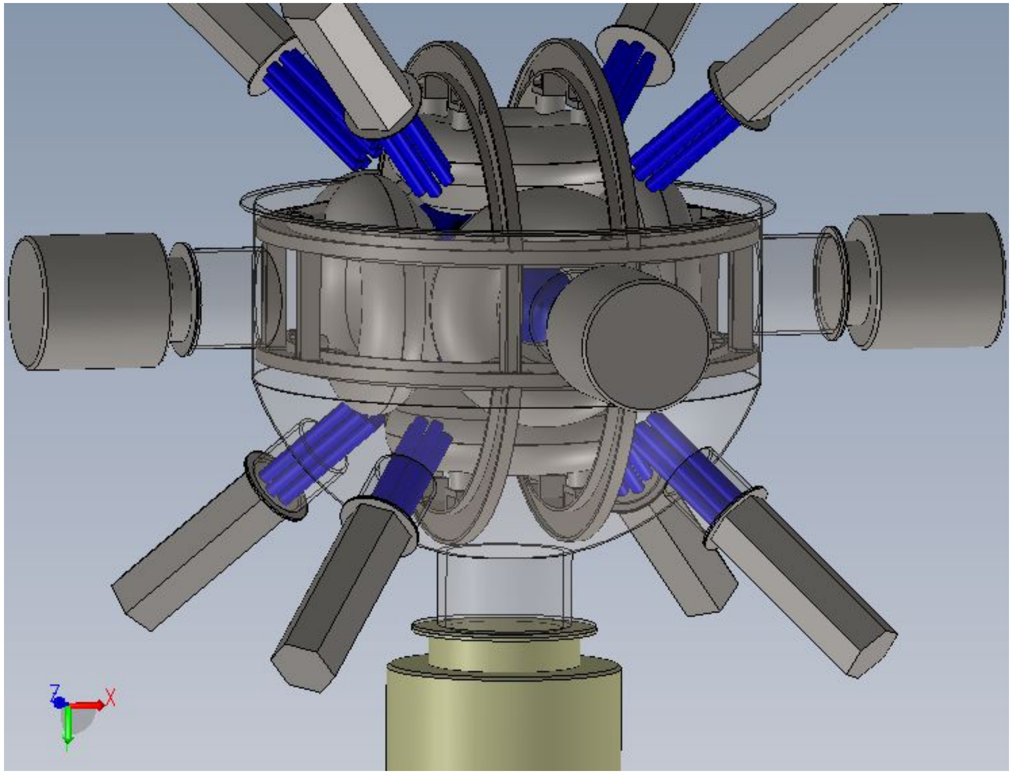

- Sustained high β operation (~ 5 ms)
- Demonstration of ion heating (>10 kV) by e-beam injection
- Verify Grad's cusp scaling

<u>3 year, $25-30M program to complete proof-of-principle</u>

Success will be defined by 1) high energy electron confinement within a factor of 10 from Grad's conjecture and 2) minimum 30% ion heating efficiency via e-beam.

Teller's Comment on Beta

" The qualitative properties of the plasma depend on the ratio of pressures in the plasma and the magnetic field. The former is the plasma pressure p, the latter $B^2/8\pi$. The ratio of the two quantities $8\pi p/B^2$ is known as β. In general, **the plasma behavior is most simple for low-β values and most interesting for high-β values**."

Teller, page 13-14, "Fusion ,Volume 1, Part A: Magnetic Confinement, edited by Edward Teller, 1981

Supplemental Slides

Electrostatic Fusion

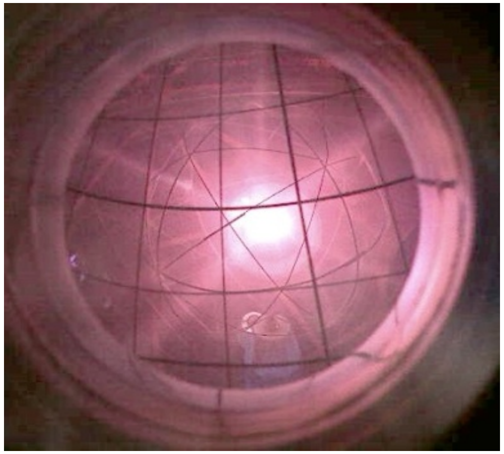

Contributions from Farnsworth, Hirsch, Elmore, Tuck, Watson and others

Operating principles

(virtual cathode type)

- e-beam (or grid) accelerates electrons into center
- Injected electrons form potential well
- Potential well accelerates/confines ions
- Energetic ions generate fusion near the center

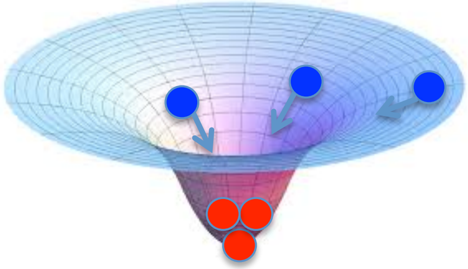

Deep negative potential well (1) accelerates and traps positive ions (2) until they generate fusion reactions

Attributes

- **Excels in generating energetic ions with good confinement**
- But loss of high energy electrons is too large

Net power generation is unlikely (present efficiency:1-10x10^{-6})

Question on Plasma Stability

Reference: "Project Sherwood: The U. S. Program in Controlled Fusion" by Bishop (1958).

• Question on Plasma Stability by Teller in 1954

- "Attempts to contain a plasma as somewhat similar to contain jello using rubber bands"
- Basis of interchange instability (plasma version of Rayleigh Taylor instability) and idea of "good curvature" vs. "bad curvature"

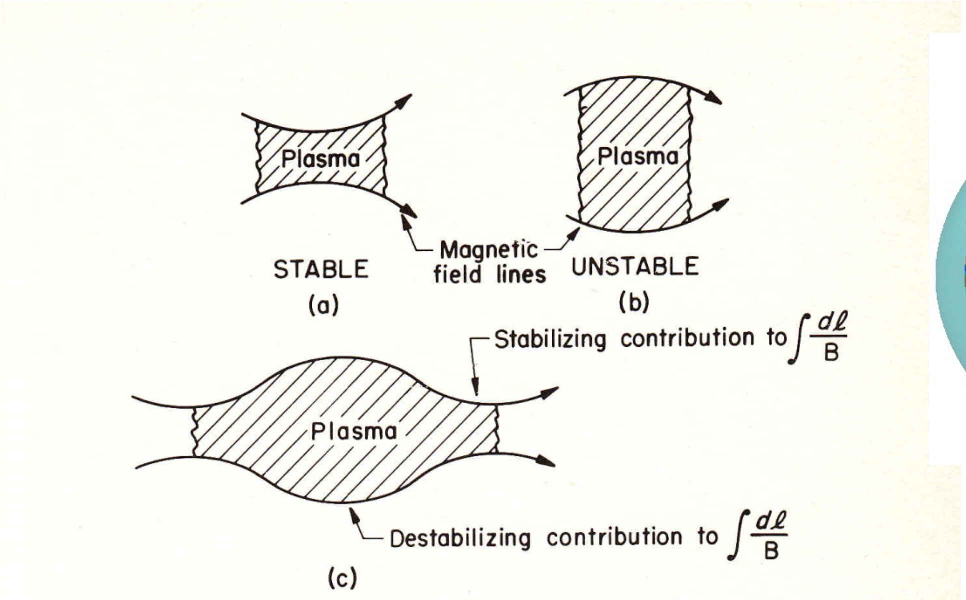

From Principles of Plasma Physics
Krall & Trivelpiece (1973)

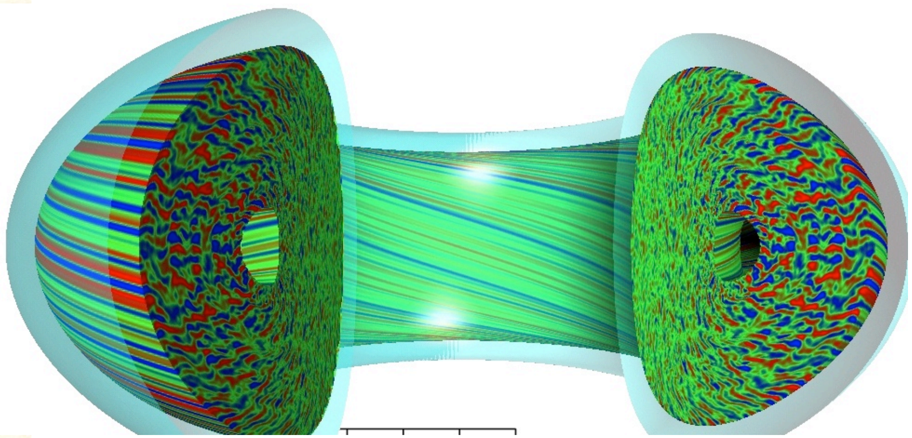

Stronger instability shown in an outer part of torus
"Tokamak ballooning mode instability"
from General Atomics Gyrokinetic simulation

Experimental Setup
for high β cusp confinement

LaB_6 Electron Gun
(7 keV, 1 – 3 A)

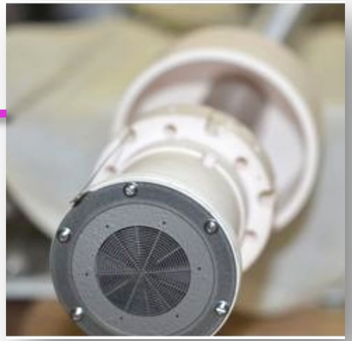

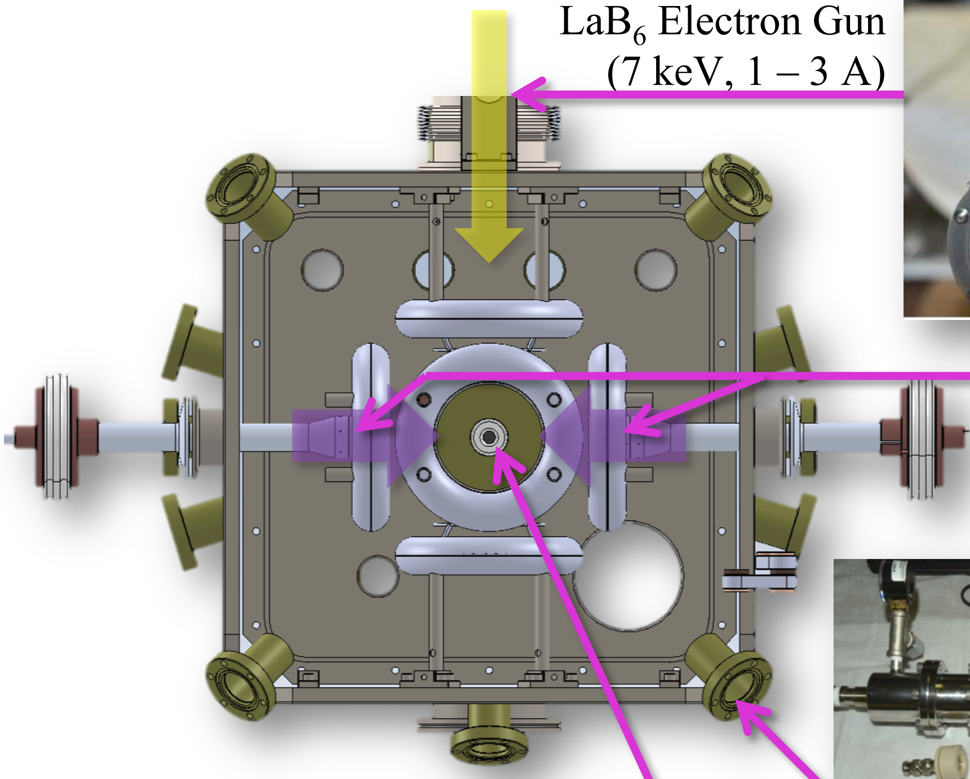

Plasma Gun
(300 MW solid arc)

X-ray diode
(2 keV x-rays and up, corner and face views)

Chamber size: 45 cm cube, Coil major radius; 6.9 cm
Distance between two coils: 21.6 cm, B-field at cusp (near coil center) 0.6 – 2.7 kG

Experimental Setup (continued)

Laser Interferometer
(532 nm, 10^{15} -10^{17} per cc)

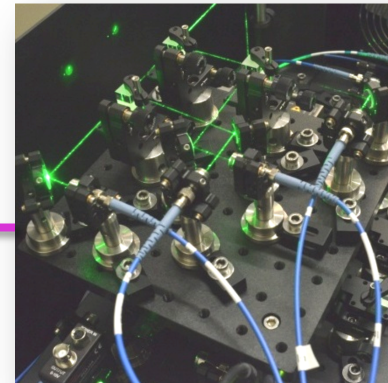

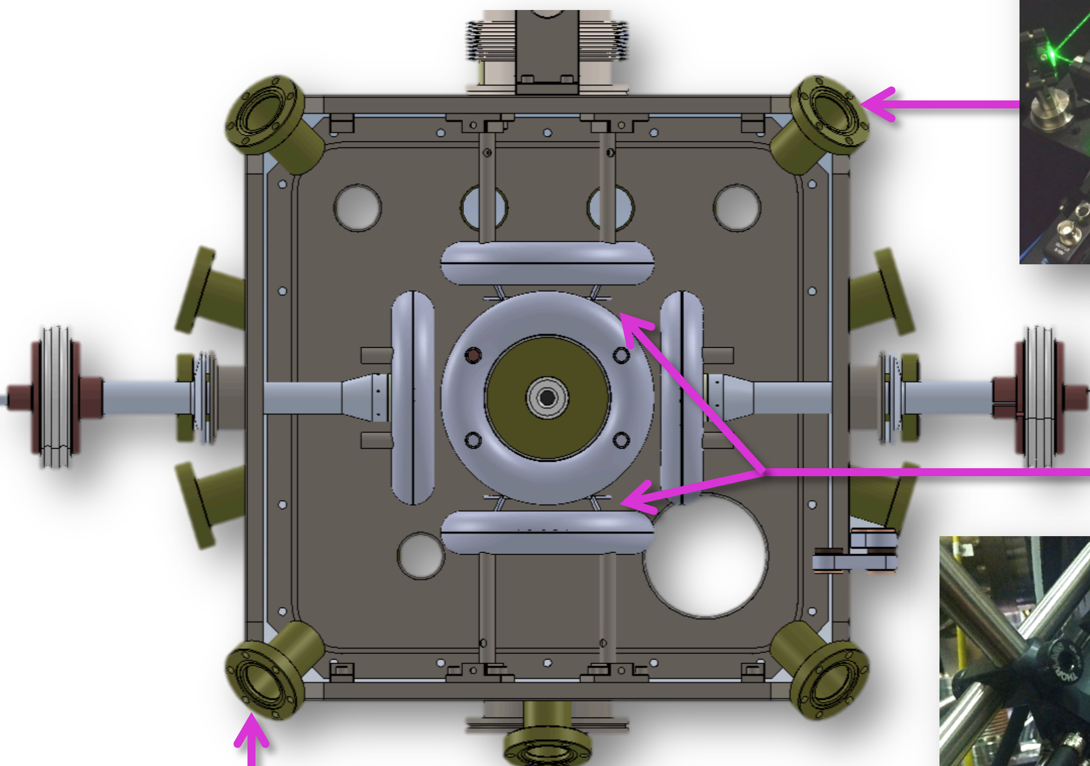

Magnetic Flux Loops

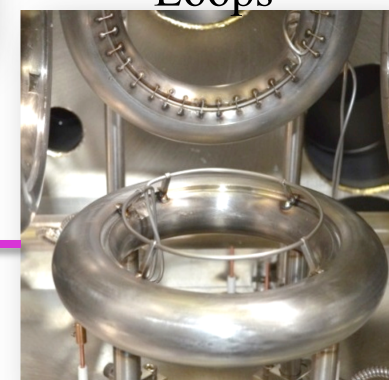

Photodiodes and Spectrometer
(Filtered for H_{α} and $C_{I\text{-}II}$, High resolution spectrometer, fiber coupled)

Solid arc plasma injector

Plasma injection by co-axial guns (j x B) using solid fuel

- Ignitron based pulse power system (40 μF cap holds 3 kJ at 12kV)
- ~100 kA arc current → ~300 MW peak power and ~7 μs pulse
- $\beta=1$@ 2.5 kG: $1.5\text{x}10^{16}$ cm^{-3} at 10 eV or 100J in a 10 cm radius sphere

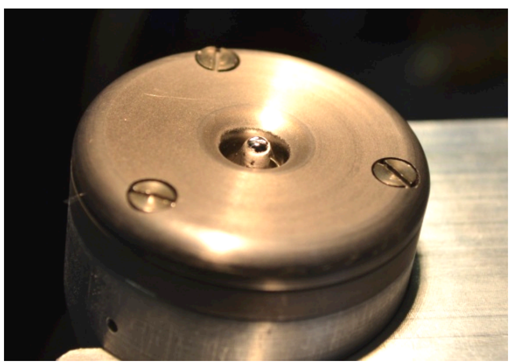

solid arc using
polypropylene film
2 mm A-K gap

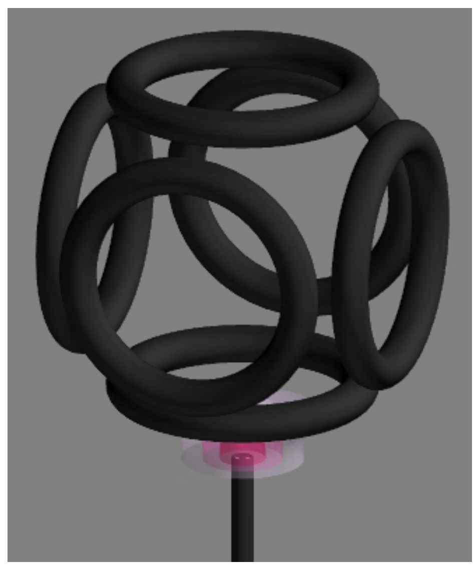

Animation of plasma injection

Dual arc plasma injection movie

High β plasma formation (two plasma guns)

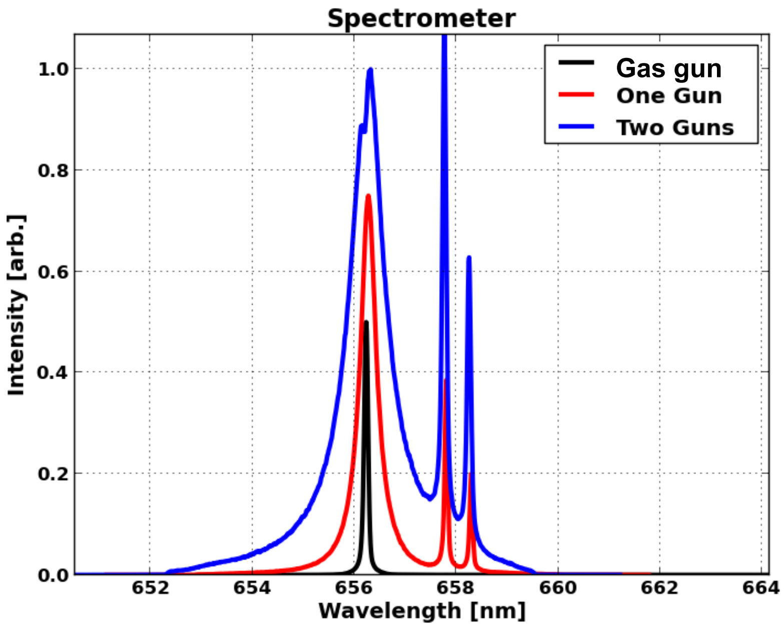

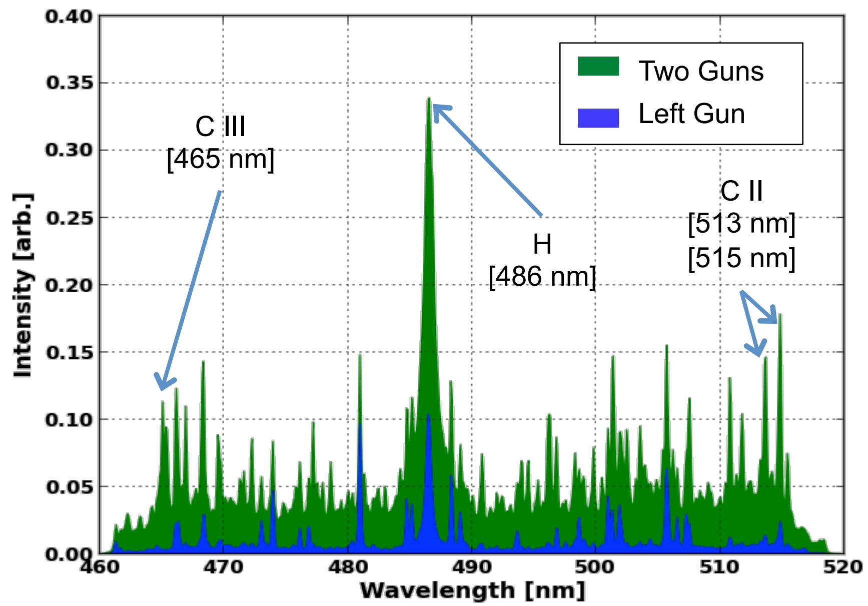

- Plasma density on the order of 10^{16} cm^{-3} from Stark broadening of Hα line
- Laser interferometer provides single shot line integrated density variation in time

- Electron temperature is estimated ~ 10 eV from C II and CIII emission
- Hα, C II line by photodiode and visible spectra by gated CCD is used to monitor T_e variation in time

High energy electron beam produces hard x-rays

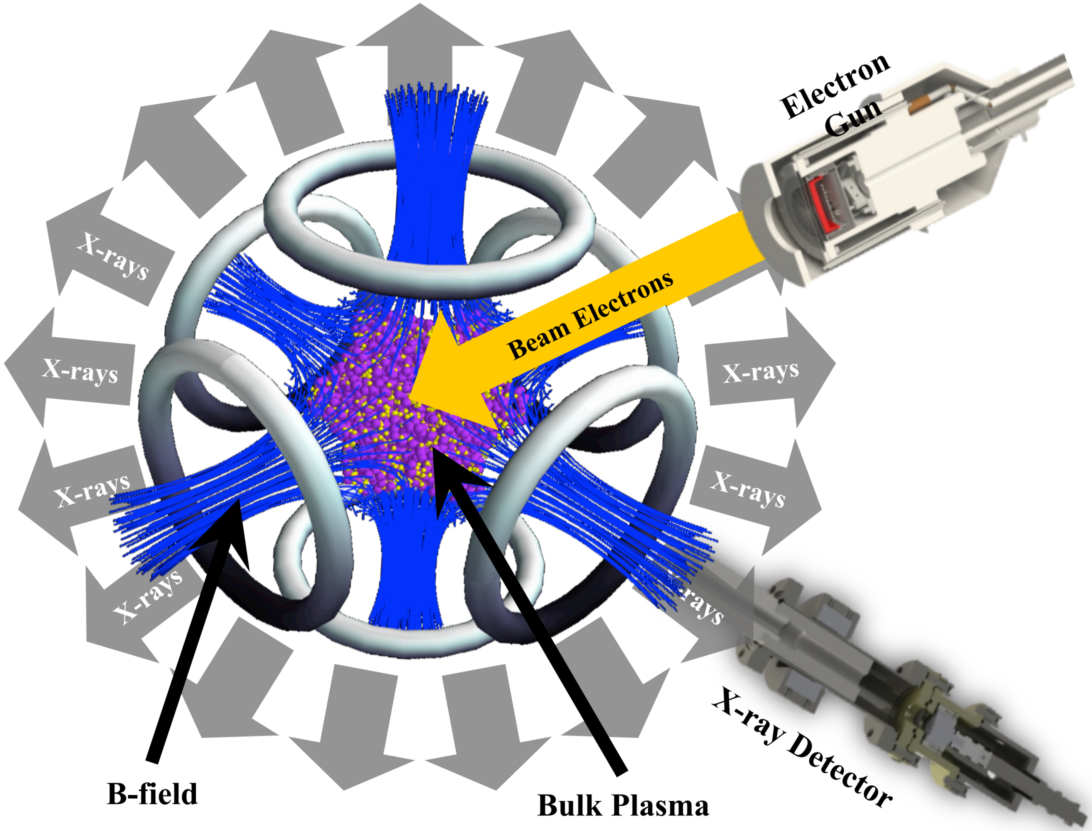

E-gun injects

Beam Electrons (7 keV)

Beam electron confinement by Cusp magnetic fields

Collisions with bulk plasma create hard x-rays (E > 2 keV) via Bremsstrahlung

Transit time: ~7 ns for 7 keV electron for 22 cm transit

Expected confinement time: ~45 ns for low β and ~18 μs for high β (x400 increase)

Bremsstrahlung x-ray emission
from interaction between beam electrons and plasma

Bremsstrahlung radiation from e-beam interaction with plasma ions

e + ion → e + ion + hν ⇒ $P^{Br} \propto n_e^{beam} E_{beam}^{1/2} n_{ion} Z_{eff}^{\,2}$

Bremsstrahlung x-ray intensity
→ <u>Direct measurement of beam e-density inside Cusp</u>

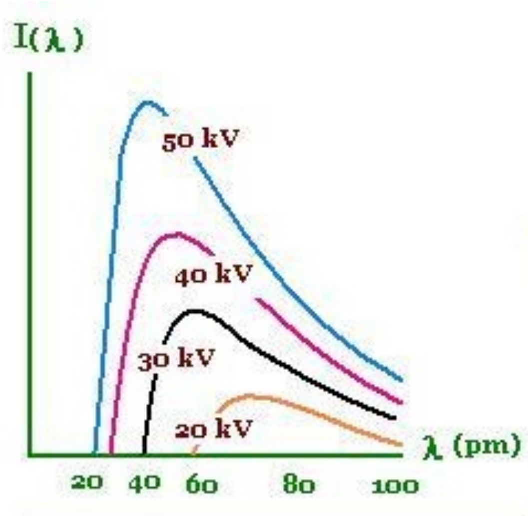

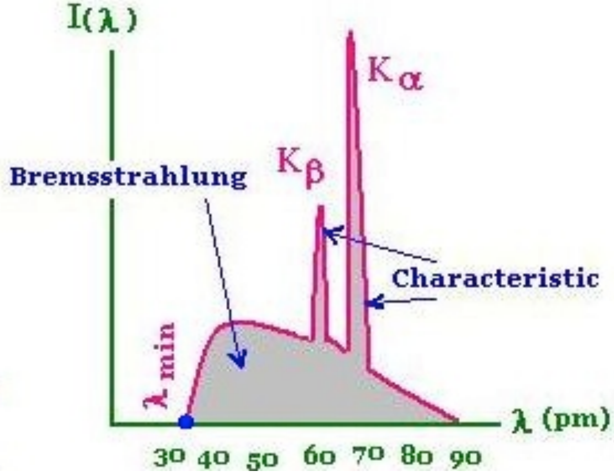

Typical beam target x-ray spectrum

Careful measurement is required to eliminate spurious radiation from impurities, vacuum wall, coil surfaces, and characteristic line emission

X-ray collecting optics to eliminate unwanted signals

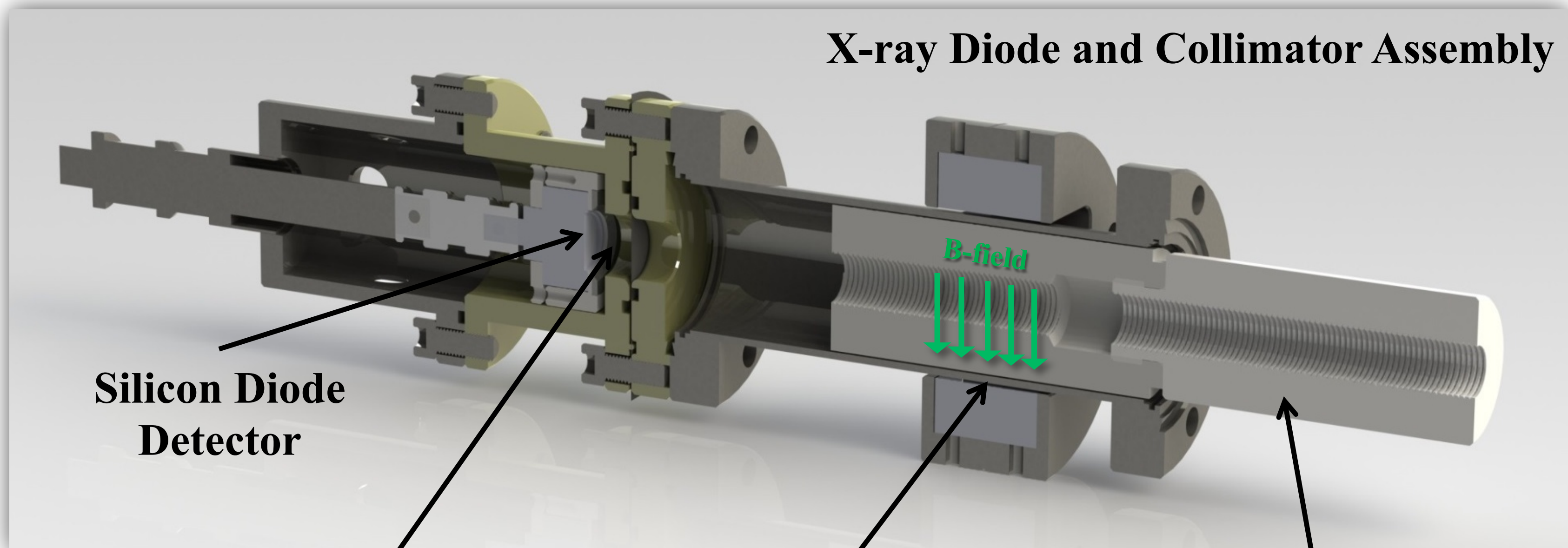

Kapton-Black Film
- Blocks plasma
- Blocks soft x-rays
- Blocks visible light

Magnetic Yoke
- Blocks beam electrons

Collimator Tube
- Limits view to plasma
- Plastic material minimizes x-ray production inside tube

Hard x-ray filter

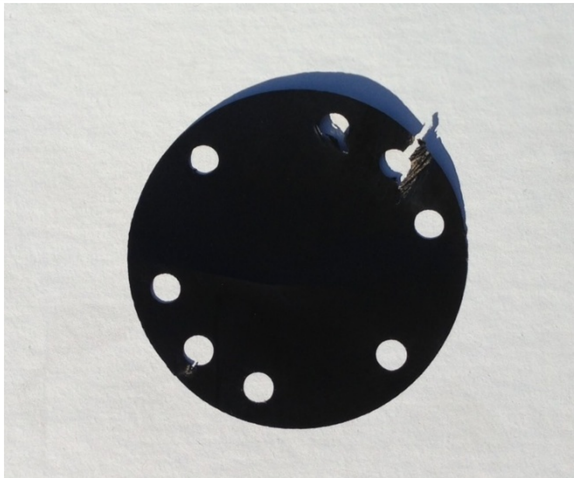

25 μm thick light tight Kapton filter
(works as vacuum interface)

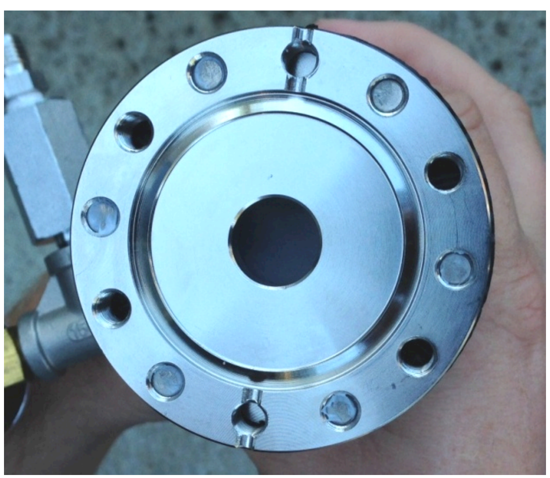

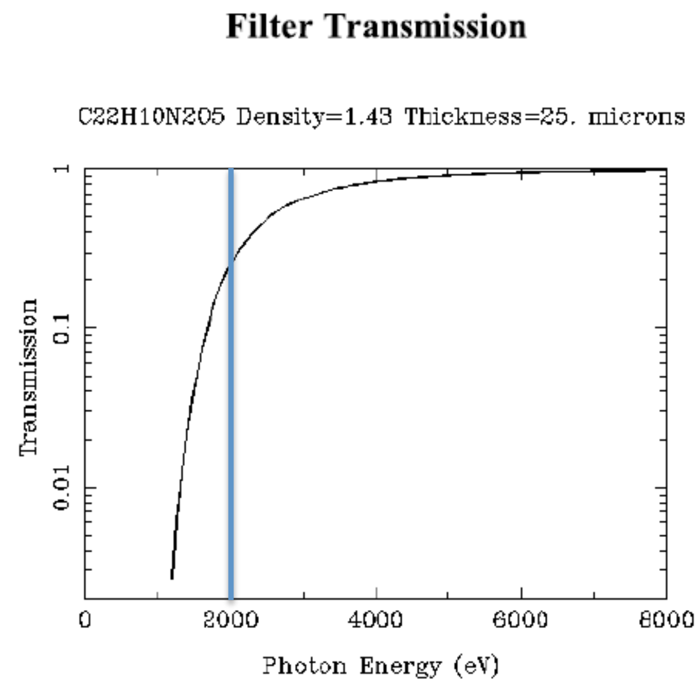

Filter has sharp cutoff at ~2 keV photon energy

→ blocks any characteristic x-ray emission from light elements up to ^{14}Si and ^{15}P
→ blocks UV-visible light from plasmas
→ blocks charged particles from reaching the detector

Confirmation of X-ray filter vs. beam energy

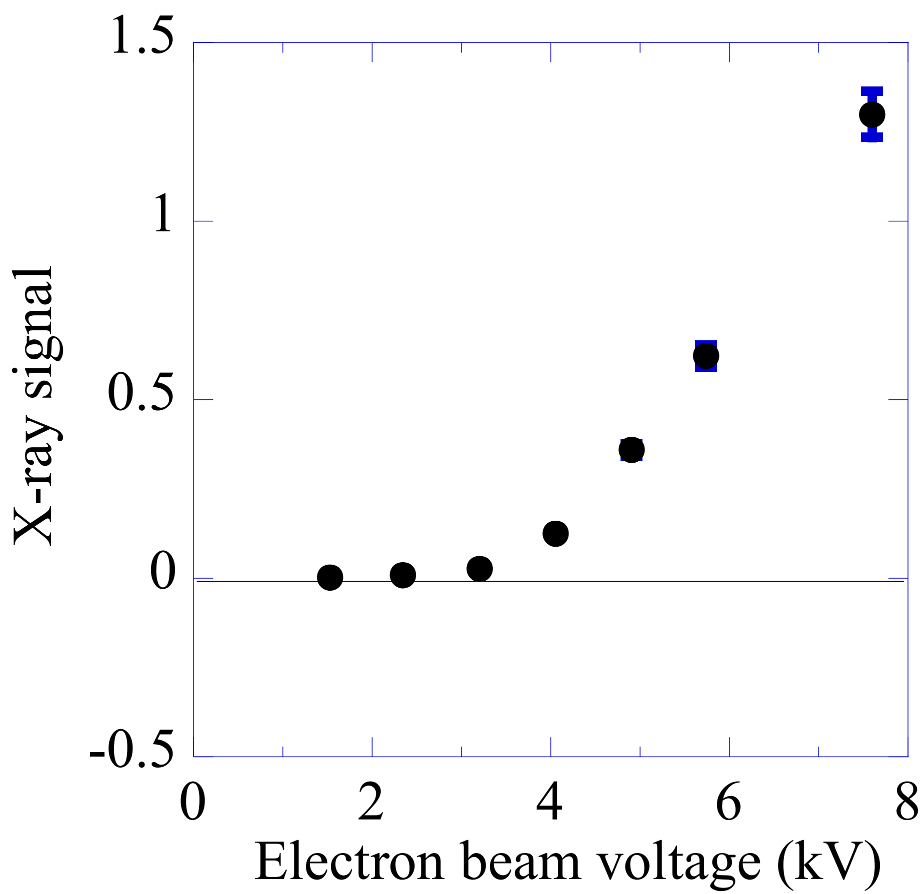

• X-ray was generated by electron beam on Stainless Steel target

• 25 μm thick Kapton filter works well to eliminate X-ray photons below 2 keV

Spatial collimation of x-ray detectors

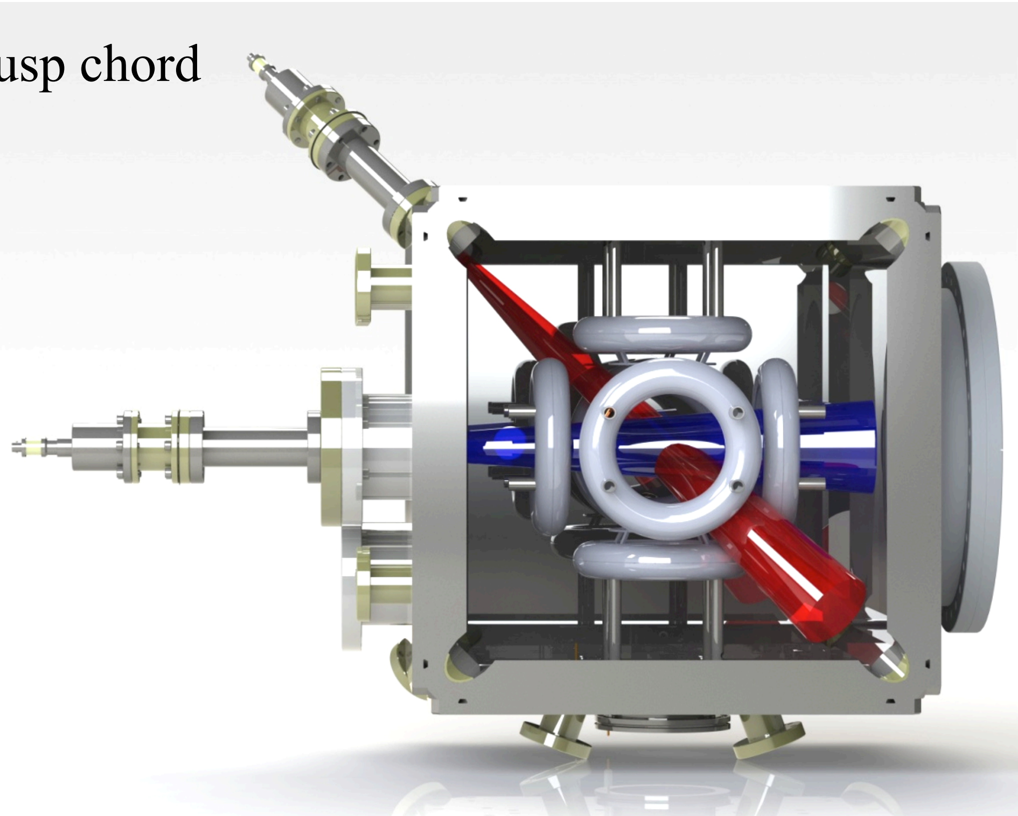

- Collimation is designed to eliminate direct line-of-sight view of metal surfaces
- In addition, opposite sides of the chamber wall are covered using Kapton film and quartz window
- Both chords allow good volume averaging of x-ray emission from core plasmas

Confirmation of X-ray collimation

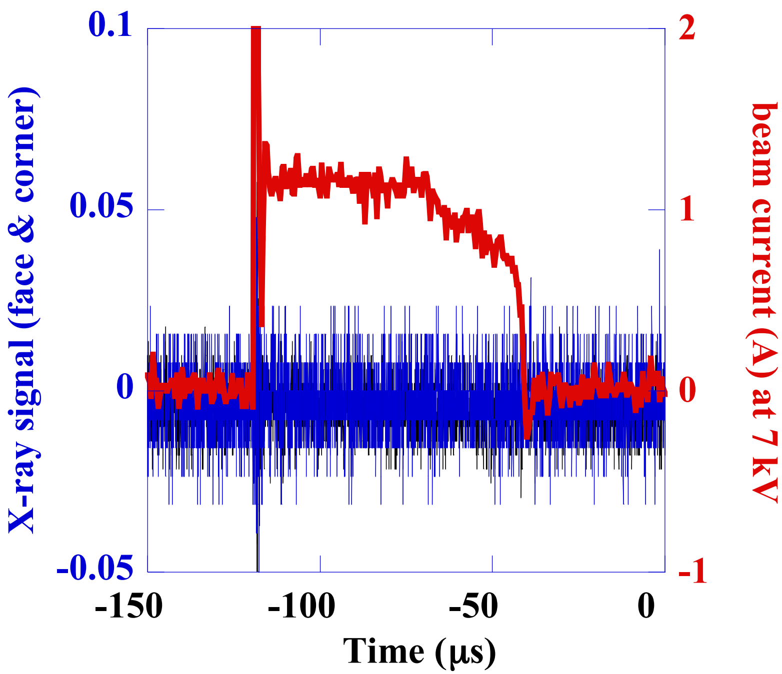

- e-beam into vacuum magnetic field (no plasma) generates no x-ray response from the diode detector
- Indication of well collimated x-ray optics

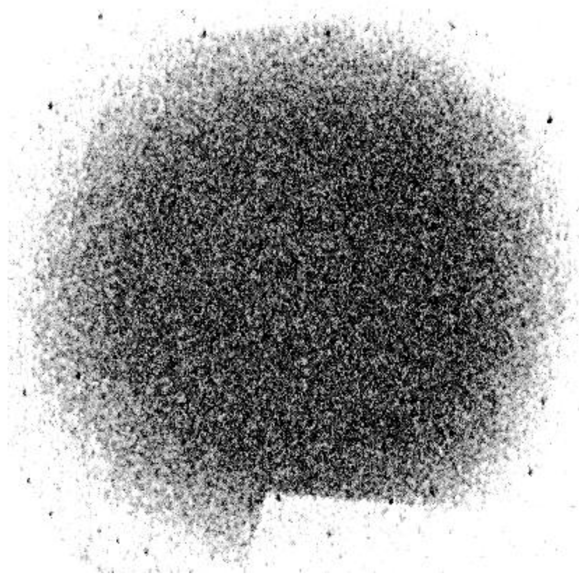

Image plate (x-ray film) exposure at the face cusp detector location

- Uniform exposure
- No sign of spatial structure from coils & walls

-10 mTorr N_2 gas target

- 20 ms exposure with 4A@7 kV e-beam
- B-field at 1.4 kG

Reproducibility of high β cusp confinement

6 consecutive shots with ~ 200 J of injected plasma energy at 2.7 kG B-fields
→ Estimated cusp beta ~ 0.7 from line averaged density at T_e ~ 10 eV

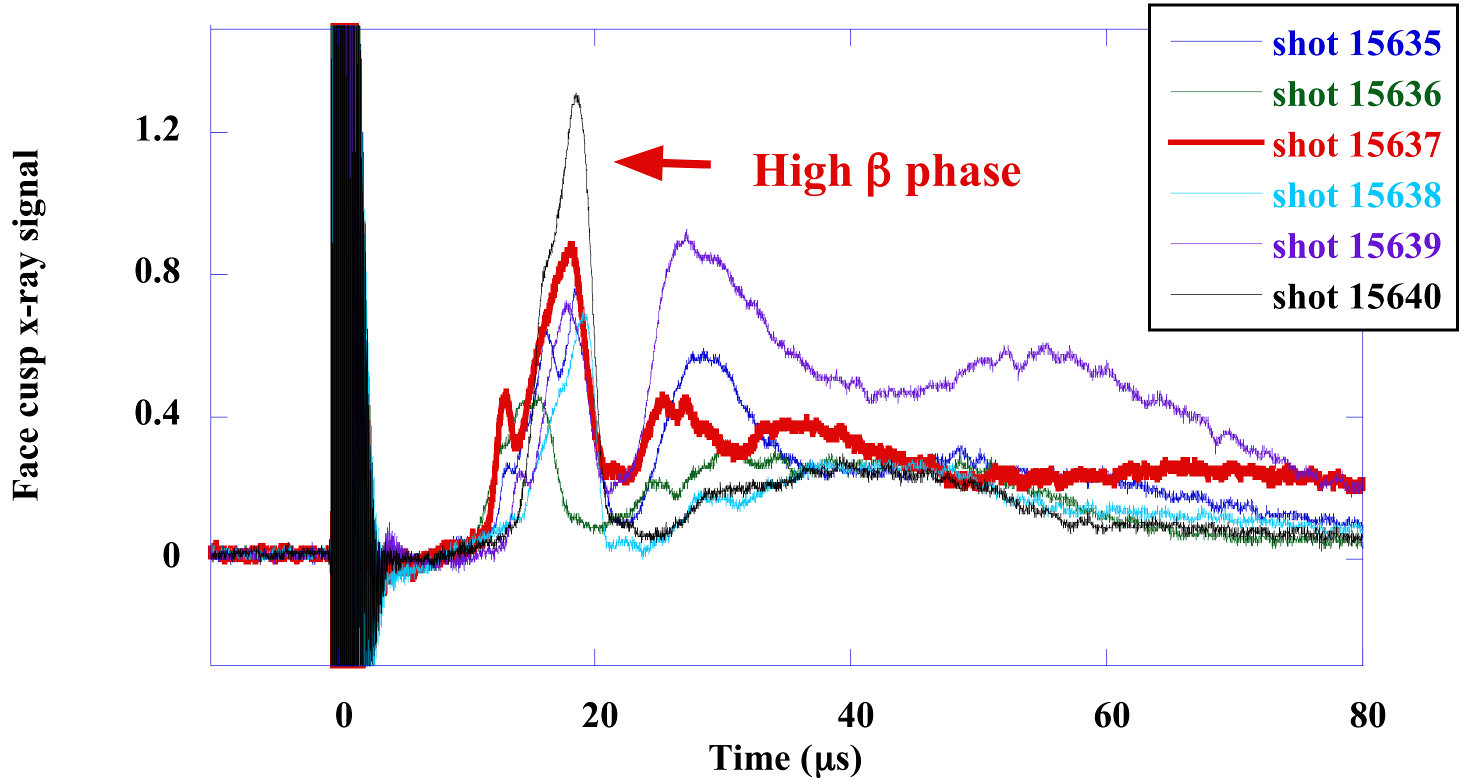

All six shots show distinctive high β phase → good reproducibility

Time averaged plasma images

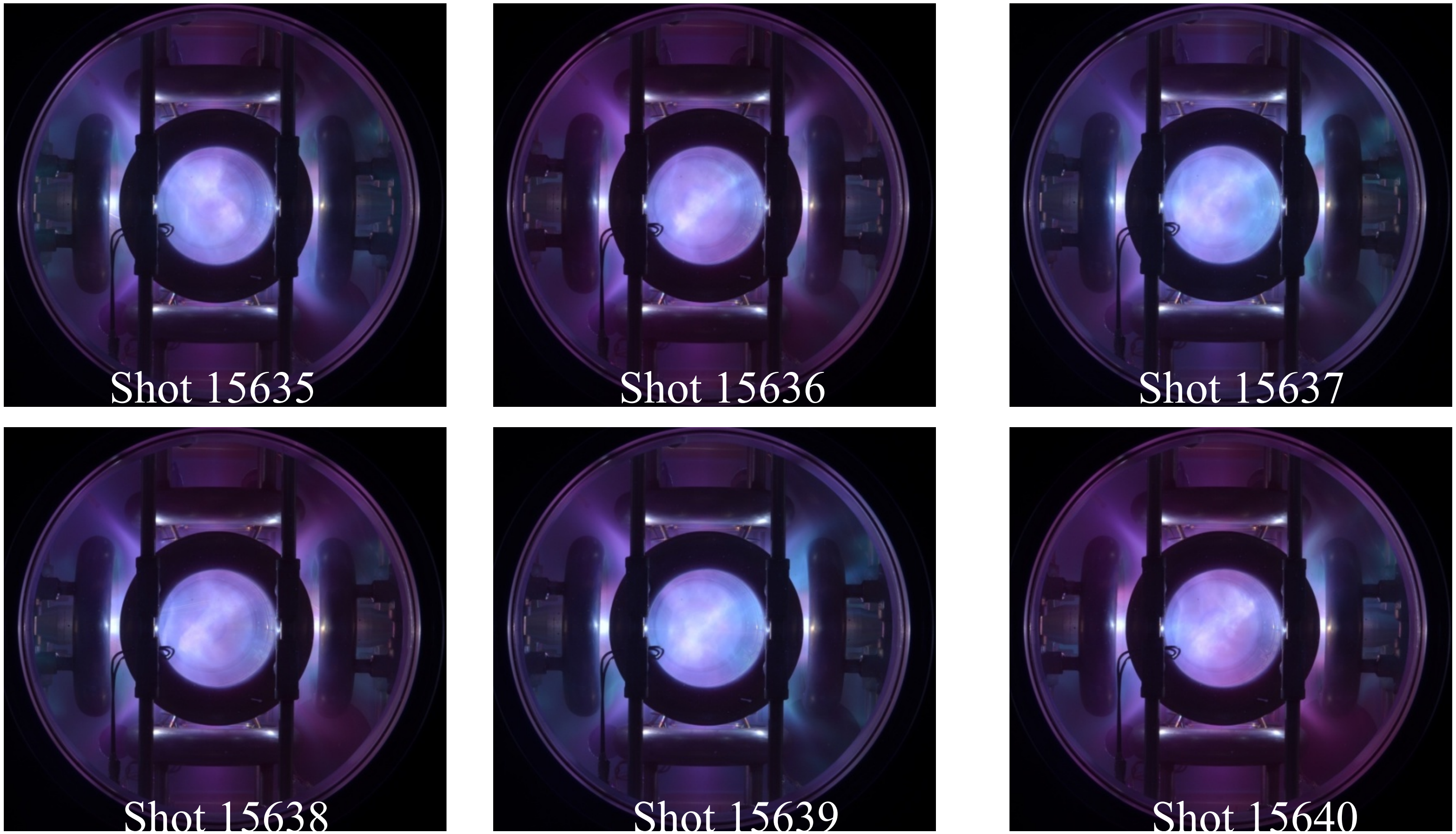

High β cusp formation: intense plasma in the core region

Time resolved spectroscopy on W-impurity

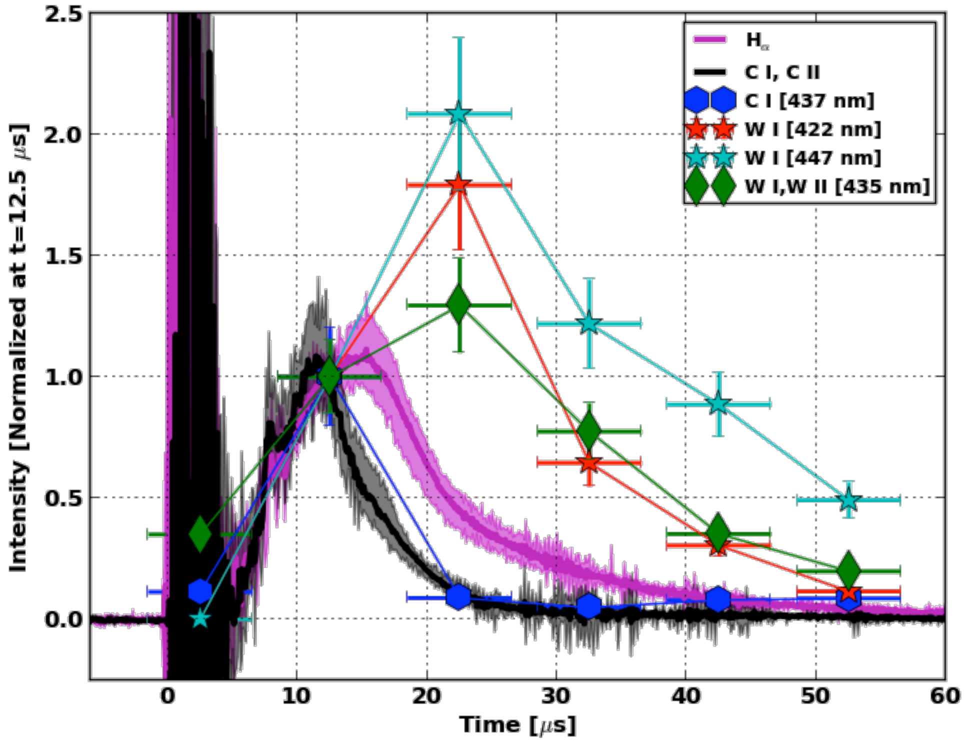

Tungsten cathode after 200 shots

• Line emission intensities from main ion species (H and C) decay early

• Despite plasma density decay (& cooling of plasma), Tungsten line intensities peak later in time and decay slowly --> indicates gradual build up of Tungsten impurity.

--> **x-ray peak late in the shot (40-50 μs) is from e-bam interaction with Tungsten**

Time resolved spectroscopy for impurity transport

Visible emission spectrum between 12 μs and 20 μs

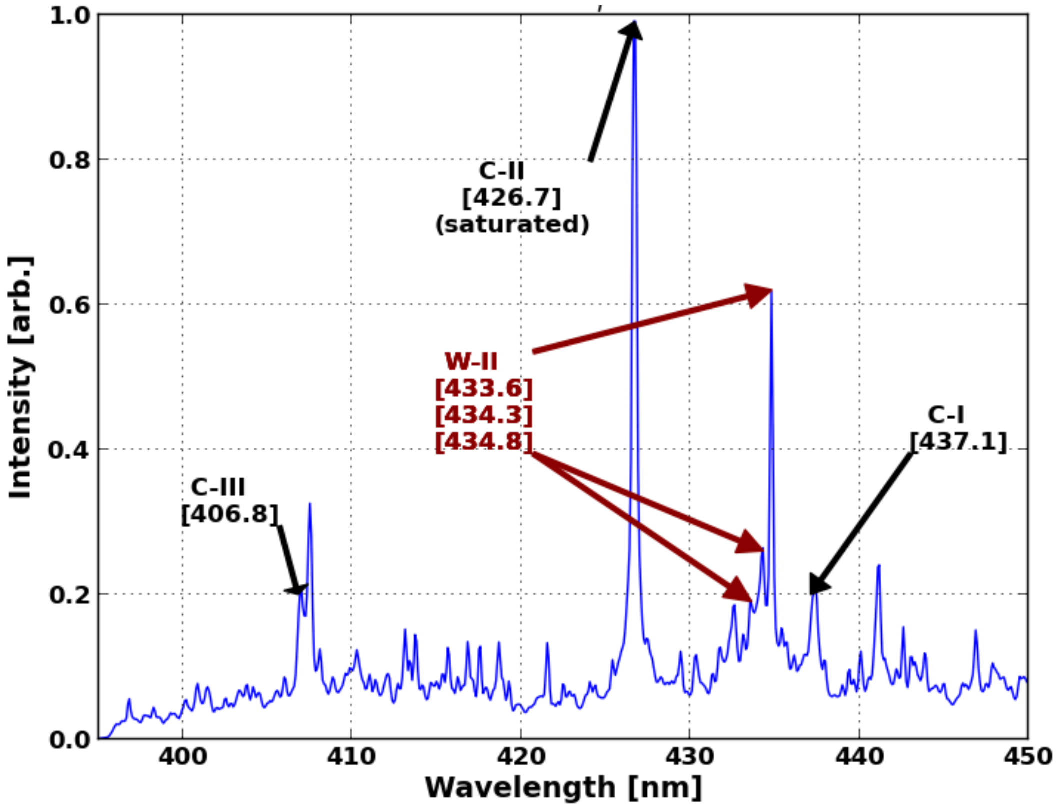

<u>During the high β phase, plasma emission shows strong C^+ lines & presence of W^+ lines</u>

(Note that avg. $n_e \sim 1.5 \times 10^{16}$ cm^{-3} and $T_e \sim 10$ eV during this period)

Time resolved spectroscopy (cont.)

Visible emission spectrum between 42 μs and 50 μs

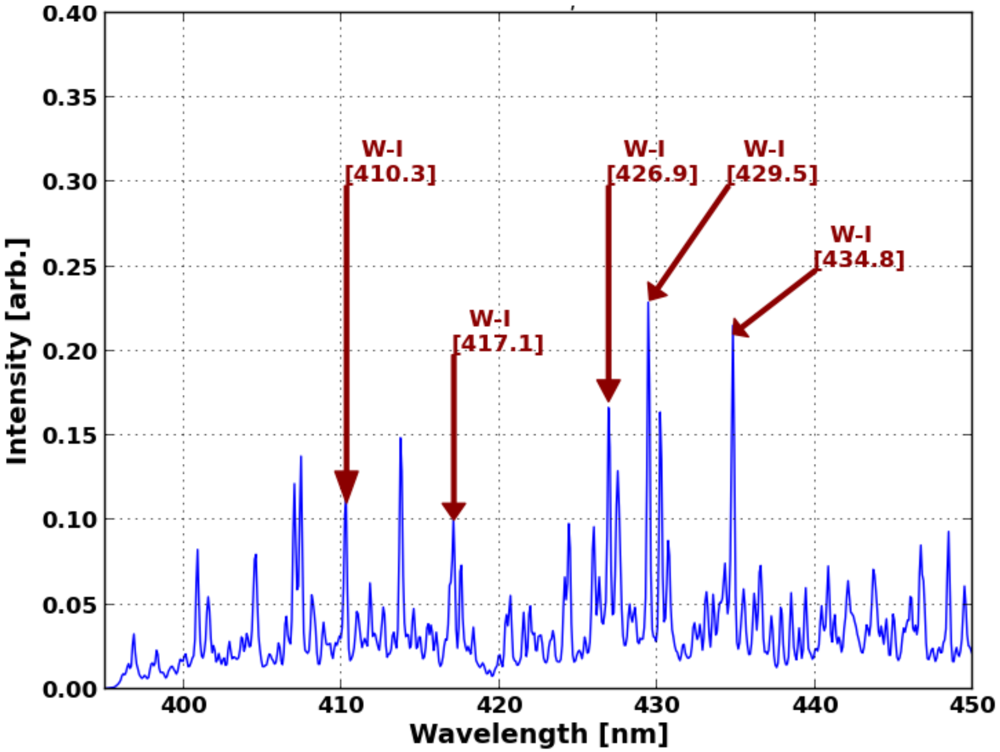

At later time, plasma emission is dominated by W neutral lines, while C^+ and W^+ lines disappear (Note that avg. $n_e \sim 0.2 \times 10^{16}$ cm^{-3} and $T_e < 10$ eV)

Estimate of High β Confinement Time

Theoretical model
to estimate high β confinement time

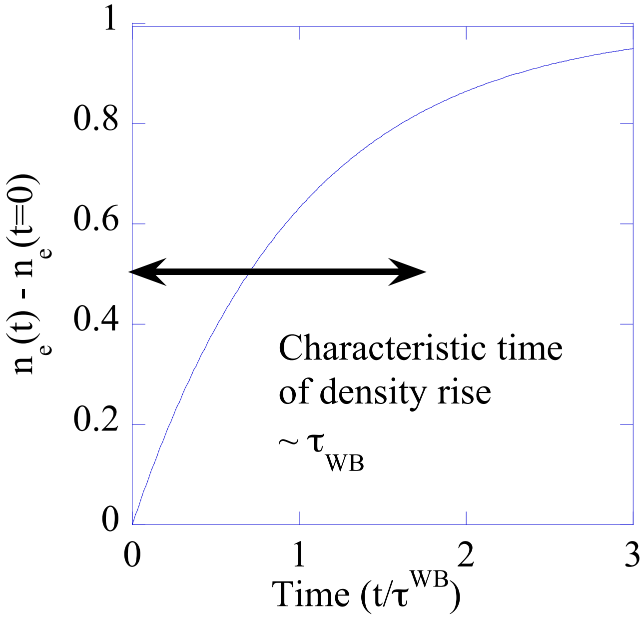

Experimental results
Shot 15640

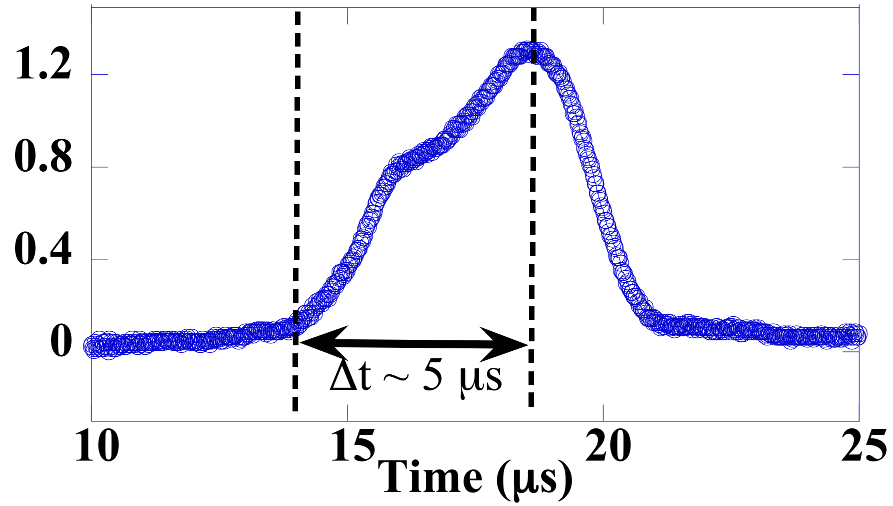

- Note the shape of x-ray intensity profile: a gradual rise and a rapid drop
- From time response of x-ray signal → τ >2.5 μs (2x τ ~ x-ray signal rise time)
- **2.5 μs is about ~ 50 times better than low β cusp confinement time**
- The observed confinement enhancement is very significant and compares well with the theoretically predicted high β cusp confinement time by Grad and his team

Unresolved issues on high β cusp

1. Decay of good confinement phase

- Decay mechanism: plasma loss/plasma cooling or magnetic field diffusion or something else
- How to extend high β state and prevent the decay

2. Topological information on cusp magnetic fields during high β state

- Thickness of transition layer
- Magnetic field lines near the cusp openings